Chapter 2
Fundamentals of Compartmental Kinetics*

2.1 Definition of Relaxation Constants

The key to tracer kinetic analysis is the concept of compartment, a group of atoms or molecules which behave in such an identically predictable manner that the introduction of a few additional but labeled atoms or molecules does not change the behavior significantly. Compartments may be large or small but they are fundamental abstractions, regardless of their size. As such they can be said to defy the very concept they were created to represent, because they require that the contents are at equilibrium and hence allow no interactions among members.

By being relegated to the interfaces between compartments, the kinetic processes studied by tracer kinetic analysis are discontinuous and hence fundamentally at variance with the real nature of kinetic processes, which must be continuous ("distributed"). The mathematically abstract compartments can of course be widely dispersed and physically intermixed with other compartments, but the definition does not allow the members of individual compartments to interact.

Non-linear modeling of distributed processes is possible in theory, provided the measurements have the necessary power of resolution, but this is so rarely the case that distributed models often arise as assemblies of commensurately diminished compartments and as such can be regarded as extensions of the linear compartments considered here. However, the resulting nonlinear kinetics will not be examined in this text. The compartment is proof of Niels Bohr's dictum that the measurement must invalidate the measured because it ignores the quantum nature of the distribution. Its saving grace is its usefulness to the practical problems of biology.

* Adapted from Gjedde (2003) Modelling metabolite and tracer kinetics, in *Molecular Nuclear Medicine*, eds L. E. Feinendegen, W. W. Shreeve, W. C. Eckelman, Y. W. Bahk and H. N. Wagner Jr., Springer-Verlag, Berlin Heidelberg, Chap. 7, pp. 121–169, with permission from Springer-Verlag, Berlin Heidelberg.

A. Gjedde et al., *Neurokinetics: The Dynamics of Neurobiology In Vivo*,
DOI 10.1007/978-1-4419-7409-9_2,

2.1.1 Single Compartment

A group of molecules, however confined or identified, form a single kinetic compartment when their rate of escape from the compartment (also called "decay" or "relaxation") is constant and proportional to the number of remaining molecules. In this sense, the compartment is an abstraction never found in real life. However, in many cases, although not in all, it is an excellent approximation when the rate of exchange among the members is much faster than the rate of relaxation. This condition is believed to be fulfilled when the compartment is well-stirred. Thus, if the stirring is not vigorous enough, the compartmentation is said to fail, and the compartment collapses into smaller compartments or noncompartmental distributions. When the product of a chemical reaction forms a single kinetic compartment, the simplest precursor–product relationship obeys a linear differential equation of the form (see Chap. 1),

$$\frac{\mathrm{d}m}{\mathrm{d}t} = j - k\,m, \tag{2.1}$$

where j is the time-variable precursor influx function and k is the relaxation or rate constant. How, or to which location, the product escapes is immaterial to the definition. In this respect, the compartment is a one-dimensional construct with time as the only dimension of change. The relaxation constant is the solution to (2.1),

$$k = \frac{j}{m} - \frac{1}{m}\left(\frac{\mathrm{d}m}{\mathrm{d}t}\right), \tag{2.2}$$

where m is the mass of molecules. The equation shows that the relaxation constant k is the ratio between the influx and the compartment content at steady-state when $\mathrm{d}m/\mathrm{d}t = 0$ (Fig. 2.1).

It is important to emphasize that the relaxation creates the compartment. Neither membranes nor anatomical subdivisions contribute to the compartmentation, except to the extent that they establish or allow the relaxation. Nor is the relaxation necessarily the result of a single mechanism. Frequently, the relaxation occurs because multiple so-called first-order mechanisms combine linearly to form a single process.

The mechanisms of passive transport across membranes, enzymatic steps of metabolic pathways, and radioactive decay, all generate compartments when they decay at a constant rate (k), such that the loss of members per unit time is

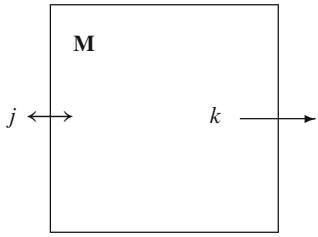

Fig. 2.1 Model of single compartment **M** occupied by the quantity m. Note that net fluxes are represented by *bidirectional arrows*, with rate constants and clearances represented by *unidirectional arrows*

proportional to the number of remaining members. Often, but not always, the number of remaining members is proportional to the concentration of the members in an aqueous medium or other solvent. The proportionality depends on several physical and chemical factors, the simplest being the volume of the solvent, but it is not always possible to judge whether they have remained constant to the satisfaction of the required proportionality between number and concentration of members.

The single isolated compartment does not exist in reality but may arise in approximation when the supply of substance is absent, instantaneous, infrequent, or unpredictable, i.e., when the function j is zero, a Dirac delta function, or when it is given only numerically.

For this compartment the transient solution to (2.1) is the convolution integral (see Chap. 1),

$$m = \mathrm{e}^{-kT}\left[m(0) + \int_o^T j\ \mathrm{e}^{kt}\ \mathrm{d}t\right], \tag{2.3}$$

where e^{-kt} is the *impulse response function*, which accounts for the monoexponentially changing loss of the original member molecules, as well as for the monoexponentially changing disappearance of new members for whom a correction must be made for the fact that they arrive at different times and hence have different risks of being expelled before a certain time. The steady-state solution to the contents of the compartment is,

$$M = \frac{J}{k} \tag{2.4}$$

in keeping with the definition of a compartment, leading to the steady-state solution to the contents of the compartment,

$$J = k\ M, \tag{2.5}$$

where variables at steady-state are given upper-case symbols.

2.1.2 Two Compartments

When two or more compartments occupy positions in series, the products have precursors which themselves form single compartments. Applying the definition, (2.1) becomes,

$$\frac{\mathrm{d}m_2}{\mathrm{d}t} = k_1\ m_1 - k_2\ m_2, \tag{2.6}$$

where m_1 refers to the precursor compartment and m_2 to the product compartment. Note that m_1 and m_2 represent numbers of molecules, usually in units of *mol* when normalized against Avogadro's number ($6 \cdot 10^{23}$). When clearance (which has unit

of flow) is the precursor's mechanism of decay, the quantity of molecules can be converted to concentration in the precursor solvent with a known volume (V_1),

$$\frac{\mathrm{d}m_2}{\mathrm{d}t} = V_1\, k_1\, \frac{m_1}{V_1} - k_2\, m_2, \tag{2.7}$$

yielding,

$$\frac{\mathrm{d}m_2}{\mathrm{d}t} = K_1\, c_1 - k_2\, m_2 \tag{2.8}$$

and

$$\frac{\mathrm{d}m_1}{\mathrm{d}t} = V_1\, \frac{\mathrm{d}c_1}{\mathrm{d}t}, \tag{2.9}$$

where K_1 symbolizes the product $V_1 k_1$ and is known as a clearance with unit of flow and c_1 is the concentration of the precursor. The clearance is the flux from compartment 1 to compartment 2 relative to the concentration. The total flux into the two compartments (and all other compartments fed by this closed system) is,

$$j_o = \sum_{i=1}^{2} \left[\frac{\mathrm{d}m_i}{\mathrm{d}t} \right] = V_1\, \frac{\mathrm{d}c_1}{\mathrm{d}t} + K_1\, c_1 - k_2\, m_2. \tag{2.10}$$

The distinction between quantity and concentration of substrate is the reason for the distinction between the rate constant k_1 and the clearance K_1. The use of concentrations instead of masses requires knowledge of the relative solvent volumes of the two compartments. For example, associating the rate constant k_1 with the concentration c_1 creates an inconsistency unless m_1 and m_2 occupy the same volume. Thus, to convert the masses included in (2.6) to concentrations, all terms are divided by the same volume, e.g., V_2, which means that the apparent concentration c_1 is really the concentration of m_1 in the solvent of $\mathbf{M}_2$, i.e., m_1/V_2, i.e. (Fig. 2.2),

$$\frac{\mathrm{d}c_2}{\mathrm{d}t} = \frac{K_1}{V_2}\, c_1 - k_2\, c_2 \tag{2.11}$$

in which the first coefficient is different from the mass balance relationship, indicating that masses and concentrations are not exchangeable, such that (2.11) and (2.12) are incompatible,

$$\frac{\mathrm{d}m_2}{\mathrm{d}t} = \frac{K_1}{V_1}\, m_1 - k_2\, m_2. \tag{2.12}$$

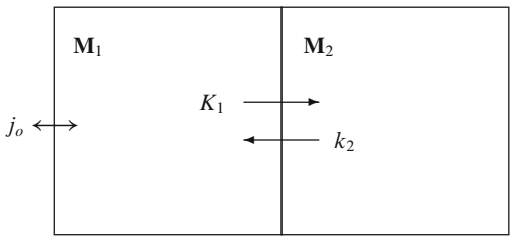

Fig. 2.2 Model of two compartments exchanging contents consisting of the product (m_2) of a reaction and m_1 is the precursor with the concentration c_1

The transiently nonlinear solution to the differential (2.6) of this relationship is again the convolution integral,

$$m_2 = \mathrm{e}^{-k_2 T}\left[m_2(0) + k_1 \int_o^T m_1\, \mathrm{e}^{k_2 t}\, \mathrm{d}t\right], \tag{2.13}$$

where k_1 is the rate constant of the reaction which converts the precursor to the product and k_2 is the rate constant for the reaction which reconverts the product to the precursor. With the substitution of c_1 for m_1, the convolution integral of (2.8) is,

$$m_2 = \mathrm{e}^{-k_2 T}\left[m_2(0) + K_1 \int_o^T c_1\, \mathrm{e}^{k_2 t}\, \mathrm{d}t\right] \tag{2.14}$$

which leads to the combined solution for m_1 and m_2 when $m_2(0) = 0$,

$$\sum_{i=1}^{2} m_i = V_1\, c_1 + K_1 \int_o^T c_1\, \mathrm{e}^{-k_2(T-t)}\, \mathrm{d}t \tag{2.15}$$

and to the combined solution for $n-1$ recipient compartments supplied by the same delivery compartment,

$$\sum_{i=1}^{n} m_i = V_1 c_1 + \sum_{h=1}^{n-1} K_{1_h} \int_o^T c_1\, \mathrm{e}^{-k_{2_h}(T-t)} \mathrm{d}t. \tag{2.16}$$

A transient multilinear expression for the net flux across the interface is obtained by integration of (2.8),

$$j_1 = K_1\, c_1 - k_2 m_2 = K_1 c_1 - K_1\, k_2 \int_o^T c_1\, \mathrm{d}t + (k_2)^2 \int_o^T m_2\, \mathrm{d}t, \tag{2.17}$$

where j_1 is the flux between compartments $\mathbf{M}_1$ and $\mathbf{M}_2$, which yields the total accumulation in the two compartments at the time T. By simple integration when $m_1(0) = m_2(0) = 0$,

$$m_2 = K_1 \int_o^T c_1\, \mathrm{d}t - k_2 \int_o^T m_2\, \mathrm{d}t \tag{2.18}$$

and, using $m_1 = V_1 c_1$, the total content as a function of the concentration in compartment 1 ($\mathbf{M}_1$) may be written as:

$$\sum_{i=1}^{2} m_i = V_1\, c_1 + (K_1 + k_2 V_1) \int_o^T c_1\, \mathrm{d}t - k_2 \int_o^T \sum_{i=1}^{2} m_i\, \mathrm{d}t. \tag{2.19}$$

For $k_2 = 0$, (2.19) becomes,

$$\sum_{i=1}^{2} m_i = V_1\, c_1 + K_1 \int_o^T c_1\, \mathrm{d}t \tag{2.20}$$

which, when divided by c_1 becomes the equation underlying the Gjedde–Patlak plot (Gjedde 1981a),

$$\sum_{i=1}^{2} v_i = V_1 + K_1 \int_o^T \frac{c_1}{c_1(T)}\, \mathrm{d}t, \tag{2.21}$$

where $v_i(T)$ is an expanding "virtual" volume and $\int_o^T c_1 \mathrm{d}t / c_1$ is an expanding "virtual" time, useful to physiologists (Sarna et al. 1977). For $k_2 > 0$, the steady-state solution to (2.6) is,

$$M_2 = \frac{k_1}{k_2}\, M_1$$

while the steady-state form of (2.15), obtained by setting derivatives to zero in (2.7) through (2.10), is,

$$\sum_{i=1}^{2} M_i = \left[V_1 + \left(\frac{K_1}{k_2} \right) \right] C_1, \tag{2.22}$$

where V_1 is the distribution volume of the molecules in compartment $\mathbf{M}_1$ and K_1/k_2 defines an additional volume V_e as a "partition volume." The size of the partition volume is dictated by the magnitudes of K_1 and k_2 and is different from the distribution volume of the molecules in compartment $\mathbf{M}_2$ (V_2). The total volume of distribution is, therefore, $V_1 + (K_1/k_2)$.

At steady-state, by definition, the flux between the compartments is nil,

$$J_1 = K_1 C_1 - k_2 M_2 = 0 \tag{2.23}$$

showing that this "system" of two compartments does nothing more than regulate the magnitude of compartment $\mathbf{M}_2$: The steady-state size of $\mathbf{M}_2$ follows passively from the unidirectional fluxes across the interface, as shown by (2.12).

2.1.3 Two Compartments with Sink

To regulate a steady-state flux without changing the size of compartment $\mathbf{M}_2$, a diversion must be established for the efflux. The receptacles of the efflux from a compartment are known as sinks. A compartment may have multiple sinks and still fulfill the criteria of compartmental behavior, as shown in the model underlying the linked differential equations (Fig. 2.3),

$$\frac{\mathrm{d}m_1}{\mathrm{d}t} = V_1\, \frac{\mathrm{d}c_1}{\mathrm{d}t} \tag{2.24}$$

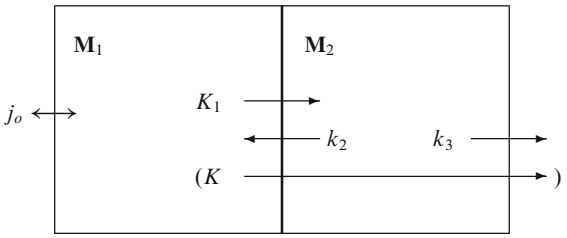

Fig. 2.3 Model of precursor and product compartments with sink. At steady-state, the sink defines a single steady-state clearance, K, equal to $K_1k_3/(k_2 + k_3)$, which reaches K_1 when $k_3 \gg k_2$

and

$$\frac{\mathrm{d}m_2}{\mathrm{d}t} = K_1\, c_1 - (k_2 + k_3)\, m_2, \tag{2.25}$$

where K_1 as the product V_1k_1 is the clearance with unit of flow and c_1 is the concentration of the precursor in the volume V_1. The total flux into the system of compartments, and all other compartments fed by it, is given by an equation identical to (2.10),

$$j_o = V_1\, \frac{\mathrm{d}c_1}{\mathrm{d}t} + K_1\, c_1 - k_2\, m_2. \tag{2.26}$$

The content of $\mathbf{M_2}$ is given by the transiently nonlinear solution,

$$m_2 = \mathrm{e}^{-(k_2+k_3)T} \left[m_2(0) + K_1 \int_o^T c_1\, \mathrm{e}^{(k_2+k_3)t}\, \mathrm{d}t \right] \tag{2.27}$$

which yields the combined solution for $m_2(0) = 0$,

$$\sum_{i=1}^{2} m_i = V_1\, c_1 + K_1 \int_o^T c_1\, \mathrm{e}^{-(k_2+k_3)(T-t)}\, \mathrm{d}t. \tag{2.28}$$

The flux into the sink at any time is given by the transiently multilinear expression,

$$j_2 = k_3\, m_2 = K_1k_3 \int_o^T c_1\, \mathrm{d}t - k_3\, (k_2 + k_3) \int_o^T m_2\, \mathrm{d}t. \tag{2.29}$$

Using the integral forms of (2.24) and (2.25), and assuming initial conditions are zero, an integral equation for the total, $m_1 + m_2$, may be written as follows.

$$\sum_{i=1}^{2} m_i = V_1\, c_1 + [K_1 + V_1\, (k_2 + k_3)] \int_o^T c_1\, \mathrm{d}t - (k_2+k_3) \int_o^T \sum_{i=1}^{2} m_i\, \mathrm{d}t. \tag{2.30}$$

The steady-state solution to (2.25) may be written as:

$$M_2 = \left(\frac{K_1}{k_2 + k_3} \right) C_1 \tag{2.31}$$

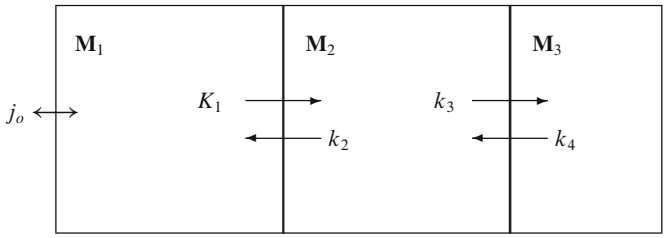

Fig. 2.4 Closed system of three compartments

which yields the steady-state flux through the system, when the content of $\mathbf{M}_2$ is inserted into (2.29),

$$J_o = k_3 M_2 = K C_1, \tag{2.32}$$

where K is the "net" clearance of the precursor from compartment $\mathbf{M}_1$ to compartment $\mathbf{M}_2$ (Fig. 2.4),

$$K = K_1 \left(\frac{k_3}{k_2 + k_3} \right) = \frac{K_1}{1 + \frac{k_2}{k_3}}. \tag{2.33}$$

2.1.4 Three Compartments

The previous system was open with a throughput. Closed compartments under normal circumstances require a return outlet as shown in the model above (Fig. 2.4), where

$$\frac{\mathrm{d}m_1}{\mathrm{d}t} = V_1 \frac{\mathrm{d}c_1}{\mathrm{d}t}, \tag{2.34}$$

$$\frac{\mathrm{d}m_2}{\mathrm{d}t} = K_1 c_1 + k_4 m_3 - (k_2 + k_3) m_2 \tag{2.35}$$

and

$$\frac{\mathrm{d}m_3}{\mathrm{d}t} = k_3 m_2 - k_4 m_3, \tag{2.36}$$

where the total flux into the three compartments is given by an equation similar to (2.10) and (2.26),

$$j_o = \sum_{i=1}^{3} \left[\frac{\mathrm{d}m_i}{\mathrm{d}t} \right] = V_1 \frac{\mathrm{d}c_1}{\mathrm{d}t} + K_1 c_1 - k_2 m_2. \tag{2.37}$$

The linked differentials (2.34–2.36) command particular attention because they underlie major applications of tracer kinetic analysis. They have been solved both for $k_4 = 0$ and $k_4 > 0$. The solutions appear complex but are easily obtained by Laplace transformation into second-order polynomials.

Transiently Non-Linear Solution to Reversible Accumulation For $k_4 > 0$, the transiently nonlinear solution to the coupled equations (2.34–2.36) is obtained in two steps. The general solution to the differential (2.36) is the ordinary convolution integral,

$$m_3 = \mathrm{e}^{-k_4 T}\left[m_3(0) + k_3 \int_o^T m_2\, \mathrm{e}^{k_4 t}\, \mathrm{d}t\right], \tag{2.38}$$

where k_3 is the rate constant of the reaction which converts the precursor in $\mathbf{M}_2$ to the product in $\mathbf{M}_3$ and k_4 is the rate constant for the reaction which reconverts this product to its precursor. When (2.38) is inserted, the solution to (2.35) for $m_2(0) = m_3(0) = 0$ is,

$$m_2 = K_1\left[\left(\frac{q_2 - k_4}{q_2 - q_1}\right)\int_o^T c_1 \mathrm{e}^{-q_2(T-t)}\mathrm{d}t - \left(\frac{q_1 - k_4}{q_2 - q_1}\right)\int_o^T c_1 \mathrm{e}^{-q_1(T-t)}\mathrm{d}t\right], \tag{2.39}$$

where

$$q_1 = \frac{k_2 + k_3 + k_4 - \sqrt{(k_2 + k_3 + k_4)^2 - 4k_2k_4}}{2} \tag{2.40}$$

and

$$q_2 = \frac{k_2 + k_3 + k_4 + \sqrt{(k_2 + k_3 + k_4)^2 - 4k_2k_4}}{2} \tag{2.41}$$

which in turn changes the form of (2.38) to

$$m_3 = \left[\frac{K_1 k_3}{q_2 - q_1}\right]\left(\int_o^T c_1\, \mathrm{e}^{-q_1(T-t)}\mathrm{d}t - \int_o^T c_1\, \mathrm{e}^{-q_2(T-t)}\mathrm{d}t\right) \tag{2.42}$$

such that the sum of the contents of $\mathbf{M}_1$, $\mathbf{M}_2$, and $\mathbf{M}_3$ now is,

$$\begin{aligned}\sum_{i=1}^{3} m_i = {} & V_1 c_1 + K_1\left(\frac{q_2 - (k_3 + k_4)}{q_2 - q_1}\right)\int_o^T c_1\, \mathrm{e}^{-q_2(T-t)}\mathrm{d}t \\ & + K_1\left(\frac{(k_3 + k_4) - q_1}{q_2 - q_1}\right)\int_o^T c_1\, \mathrm{e}^{-q_1(T-t)}\mathrm{d}t\end{aligned} \tag{2.43}$$

which expresses the general property that,

$$\sum_{i=1}^{3} m_i = V_1 c_1 + \sum_{h=1}^{2} K_{1_h}\int_o^T c_1\, \mathrm{e}^{-k_{2_h}(T-t)}\mathrm{d}t,$$

where $K_{1_1} = K_1\,[q_2 - (k_3 + k_4)]/[q_2 - q_1]$, $K_{1_2} = K_1\,[(k_3 + k_4) - q_1]/[q_2 - q_1]$, $k_{2_1} = q_2$, and $k_{2_2} = q_1$.

Transiently Non-Linear Solution to Irreversible Accumulation For $k_4 = 0$, the nonlinear solution of (2.43) reduces to the one given by Sokoloff et al. (1977), for $m_2(0) = m_3(0) = 0$,

$$\sum_{i=1}^{3} m_i = V_1\, c_1 + \frac{K_1 k_2}{k_2 + k_3} \int_o^T c_1\, \mathrm{e}^{-(k_2+k_3)(T-t)}\, \mathrm{d}t + \frac{K_1 k_3}{k_2 + k_3} \int_o^T c_1\, \mathrm{d}t \quad (2.44)$$

for which it should be kept in mind that closed systems without backflux have no obvious biological role, although they may exist under experimental circumstances for certain tracers. The solution reduces to,

$$\sum_{i=1}^{3} m_i = V_1 c_1 + K \left[\int_o^T c_1\, \mathrm{d}t + \left(\frac{k_2}{k_3} \right) \int_o^T c_1 \mathrm{e}^{-(k_2+k_3)(T-t)}\, \mathrm{d}t \right], \quad (2.45)$$

where the "net" clearance is,

$$K = K_1 \left(\frac{k_3}{k_2 + k_3} \right) = \frac{K_1}{1 + \frac{k_2}{k_3}} \quad (2.46)$$

as defined in (2.33). Gjedde (1982) showed that this equation, when normalized against the concentration c_1 at time T, defines a continuously increasing apparent volume of distribution in the manner of the Gjedde–Patlak solution to (2.19) (Gjedde 1982),

$$\sum_{i=1}^{3} v_i = \left[V_1 + \left(\frac{K_1 k_2}{k_2 + k_3} \right) \int_o^T \left[\frac{c_1(t)}{c_1(T)} \right] \mathrm{e}^{-(k_2+k_3)(T-t)}\, \mathrm{d}t \right] + K \int_o^T \frac{c_1(t)}{c_1(T)}\, \mathrm{d}t \quad (2.47)$$

if compartments $\mathbf{M}_1$ and $\mathbf{M}_2$ reach a steady balance ("secular" equilibrium), depending on the magnitudes of k_2 and k_3.

Transiently Linear Solution to Reversible Accumulation For $k_4 > 0$, the transient multilinear solution to (2.34–2.36) was given by Evans (1987) for $m_2(0) = m_3(0) = 0$,

$$\begin{aligned} \sum_{i=1}^{3} m_i = {} & a_1 c_1 + a_2 \int_o^T c_1\, \mathrm{d}t + a_3 \int_o^T \int_o^u c_1\, \mathrm{d}t\, \mathrm{d}u \\ & + a_4 \int_o^T \sum_{i=1}^{3} m_i\, \mathrm{d}t + a_5 \int_o^T \int_o^u \sum_{i=1}^{3} m_i\, \mathrm{d}t\, \mathrm{d}u, \end{aligned} \quad (2.48)$$

where,

$$\begin{aligned} a_1 &= V_1 \\ a_2 &= K_1 + V_1(k_2 + k_3 + k_4) \\ a_3 &= K_1(k_3 + k_4) + k_2 k_4 V_1 \end{aligned}$$

$$a_4 = -(k_2 + k_3 + k_4)$$
$$a_5 = -k_2 k_4.$$

Transiently Linear Solution to Irreversible Accumulation For $k_4 = 0$, the multilinear solution to (2.34–2.36) was first given by Blomqvist (1984). It is obtained here by setting $k_4 = 0$ in (2.48) for $m_2(0) = m_3(0) = 0$,

$$\sum_{i=1}^{3} m_i = V_1 c_1 + [K_1 + V_1(k_2 + k_3)] \int_o^T c_1 \, \mathrm{d}t + K_1 k_3 \int_o^T \int_o^u c_1 \, \mathrm{d}t \, \mathrm{d}u - (k_2 + k_3) \int_o^T \sum_{i=1}^{3} m_i \, \mathrm{d}t \tag{2.49}$$

Steady-State Solution to Reversible Accumulation When $k_4 > 0$, the steady-state flux (J_o) through the system is zero because of the absent sink. The transient solutions describe the time-course of the approach of each of the compartments toward steady-state. The net steady-state flux of zero is associated with the following distinct sizes of each compartment, depending on the magnitudes of the rate constants,

$$M_3 = \left(\frac{k_3}{k_4}\right) M_2 = \left(\frac{K_1 k_3}{k_2 k_4}\right) C_1 \tag{2.50}$$

and

$$M_2 = \left(\frac{K_1}{k_2}\right) C_1 \tag{2.51}$$

yielding the sum of the three compartments,

$$\sum_{i=1}^{3} M_i = \left[V_1 + \frac{K_1}{k_2}\left(1 + \frac{k_3}{k_4}\right)\right] C_1, \tag{2.52}$$

where M is the mass of molecules. The equation shows that in this closed system of three compartments, the content of one or more compartments is maintained at a specific level dictated by the magnitude of the relaxation constants. It is important to note that only the relative magnitudes of the constants matter. The steady-state volume of distribution is $\sum_{i=1}^{3} M_i / C_1$ according to (2.52) (Fig. 2.5).

Pseudo-Steady-State Solution to Irreversible Accumulation When $k_4 = 0$, the content of the last of the compartments ($\mathbf{M}_3$) continues to increase according to (2.47) and, thus, never reaches true steady-state. When $T \gg k_2 + k_3$, the "virtual" volume of distribution of (2.47) approaches a line of slope K and ordinate intercept $V_1 + K_1 k_2/(k_2 + k_3)^2$ with time. The pseudo-steady-state solution to (2.47), also known as the Gjedde–Patlak plot is (Gjedde 1982; Patlak et al. 1983),

$$\sum_{i=1}^{3} v_i(T) \cong \left[V_1 + \frac{K_1 k_2}{(k_2 + k_3)^2}\right] + K \int_o^T \frac{c_1(t)}{C_1(T)} \, \mathrm{d}t. \tag{2.53}$$

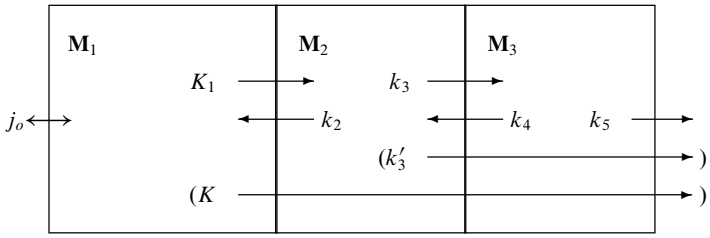

Fig. 2.5 Model of multiple compartment with multiple sinks. Steady-state k_3' equals $k_3 k_5/(k_4 + k_5)$ and reaches k_3 when $k_5 \gg k_4$. Steady-state K equals $K_1 k_3'/(k_2 + k_3')$ and reaches K_1 when $k_3' \gg k_2$ at near-equilibrium

2.1.5 Three Compartments with Sink

An open system with a throughput can be created by adding another rate constant to compartment $\mathbf{M_3}$ as shown in Fig. 2.5,

$$\frac{\mathrm{d}m_1}{\mathrm{d}t} = V_1 \frac{\mathrm{d}c_1}{\mathrm{d}t}, \tag{2.54}$$

$$\frac{\mathrm{d}m_2}{\mathrm{d}t} = K_1\, c_1 + k_4\, m_3 - (k_2 + k_3)\, m_2 \tag{2.55}$$

and

$$\frac{\mathrm{d}m_3}{\mathrm{d}t} = k_3\, m_2 - (k_4 + k_5)\, m_3 \tag{2.56}$$

with the total flux into the compartments (and all other compartments fed by this open system), equal to

$$j_o = V_1 \frac{\mathrm{d}c_1}{\mathrm{d}t} + K_1\, c_1 - k_2\, m_2. \tag{2.57}$$

The time course of the sum of the magnitudes of all three compartments is a complex solution to (54–56). An easier approach is the numerical solution obtained by simply adding the analytical solutions for the individual compartment, but the number of coefficients makes the solution less useful, and it will not be given here. More important is the net flux through the system at steady-state.

Generalized Steady-State Solution

The steady-state magnitudes of the compartments are

$$M_3 = \left[\frac{k_3}{k_4 + k_5}\right] M_2 = \left(\frac{K_1}{k_2 + k_3'}\right)\left[\frac{k_3}{k_4 + k_5}\right] C_1 \tag{2.58}$$

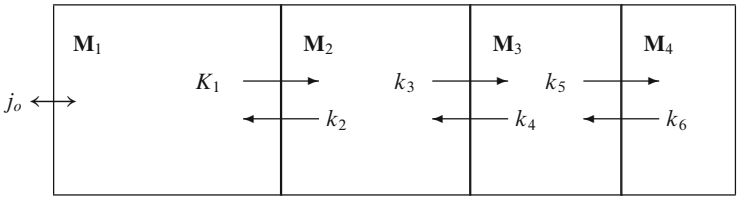

Fig. 2.6 Model of closed system of multiple exchanging compartments

and, of course,

$$M_2 = \left(\frac{K_1}{k_2 + k_3'}\right) C_1 \tag{2.59}$$

such that

$$\sum_{i=1}^{3} M_i = \left(V_1 + \left(\frac{K_1}{k_2 + k_3'}\right)\left[1 + \left(\frac{k_3}{k_4 + k_5}\right)\right]\right) C_1, \tag{2.60}$$

where the apostrophe ("prime") of the apparent relaxation constant k_3' refers to its definition as a composite of the rate constants of several compartmental interfaces affecting compartment $\mathbf{M}_3$ (Fig. 2.6),

$$k_3' = k_3 \left(\frac{k_5}{k_4 + k_5}\right). \tag{2.61}$$

The steady-state flux through the system is

$$J_o = k_5\, M_3 = K\, C_1, \tag{2.62}$$

where

$$K = \frac{K_1}{1 + \frac{k_2}{k_3}\left(1 + \frac{k_4}{k_5}\right)} = \frac{K_1}{1 + \frac{k_2}{k_3'}} \tag{2.63}$$

which can now be generalized to any number of nested compartments with a terminal sink,

$$K = \frac{K_1}{1 + \frac{k_2}{k_3}\left(1 + \frac{k_4}{k_5}\left[1 + \cdots + \left(1 + \frac{k_{2n-2}}{k_{2n-1}}\right)\right]\right)}, \tag{2.64}$$

where n is the number of compartments ending with a sink described by the rate constant k_{2n-1}. The corresponding size of the terminal compartment is given by:

$$M_n = \left(\frac{K}{k_{2n-1}}\right) C_1 \tag{2.65}$$

and the combined magnitude of all compartments is

$$\sum_{i=1}^{n} M_i = \left[V_1 + K \left(\frac{1}{k'_3} + \frac{1}{k'_5} + \frac{1}{k'_7} + \cdots + \frac{1}{k'_{2i-1}} + \cdots + \frac{1}{k_{2n-1}} \right) \right] C_1, \tag{2.66}$$

where

$$k'_{2i-1} = \frac{k_{2i-1}}{1 + \frac{k_{2i}}{k_{2i+1}} \left[1 + \frac{k_{2i+2}}{k_{2i+3}} \left(1 + \cdots + \left[1 + \frac{k_{2n-2}}{k_{2n-1}} \right] \right) \right]}. \tag{2.67}$$

2.1.6 Four or More Compartments

The serial system shown in Fig. 2.6 without a throughput can be created by adding additional compartments ($\mathbf{M_4}$-$\mathbf{M}_n$), such that the system consists of the delivery compartment,

$$\frac{\mathrm{d}m_1}{\mathrm{d}t} = V_1 \frac{\mathrm{d}c_1}{\mathrm{d}t}, \tag{2.68}$$

the precursor compartment,

$$\frac{\mathrm{d}m_2}{\mathrm{d}t} = K_1 c_1 + k_4 m_3 - (k_2 + k_3) m_2, \tag{2.69}$$

and multiple product compartments in series, including

$$\frac{\mathrm{d}m_3}{\mathrm{d}t} = k_3 m_2 + k_6 m_4 - (k_4 + k_5) m_3 \tag{2.70}$$

and, for $4 < i < n$,

$$\frac{\mathrm{d}m_i}{\mathrm{d}t} = k_{2i-3} m_{i-1} + k_{2i} m_{i+1} - (k_{2i-1} + k_{2i-2}) m_i \tag{2.71}$$

and ending with the nth compartment,

$$\frac{\mathrm{d}m_n}{\mathrm{d}t} = k_{2n-3} m_{n-1} - k_{2n-2} m_n, \tag{2.72}$$

where the total flux into the four or more compartments generalizes to,

$$j_o = \sum_{i=1}^{n} \left[\frac{\mathrm{d}m_i}{\mathrm{d}t} \right] = V_1 \frac{\mathrm{d}c_1}{\mathrm{d}t} + K_1 c_1 - k_2 m_2 \tag{2.73}$$

as the flux across interior boundaries cancels out in the sum.

Convolution of Impulse Response Function as Generalized Transient Solution

The impulse response function is the function that defines the changes of the compartmental contents with time when convolved with the input or "forcing" function, which defines the contents of the delivery compartment, be it the vascular bed or another (reference) tissue. In the case of compartments defined by linear first-order differential equations, the ratio between the integrals of the tissue curve and the forcing function, extrapolated to infinity, yields the ratio between the impulse response function coefficients K_{1_h} and k_{2_h}. Linear systems theory shows that the generalized transiently nonlinear solution to the linked differential equations (2.68–2.72), for $\sum_{i=1}^{n} m_i(0) = 0$, is the convolution of the impulse response function given in (2.16) with the vascular "forcing" function (Gunn et al. 2001),

$$\sum_{i=1}^{n} m_i = V_1 c_1 + \sum_{h=1}^{n-1} K_{1_h} \int_o^T c_1 \, \mathrm{e}^{-k_{2_h}(T-t)} \, \mathrm{d}t, \tag{2.74}$$

where the coefficients K_{1_h} define the total clearance,

$$K_1 = \sum_{h=1}^{n-1} K_{1_h} \tag{2.75}$$

and the relaxation constants k_{2_h} define the steady-state volume of distribution,

$$V = \sum_{i=1}^{n} V_i = V_1 + \sum_{h=1}^{n-1} \frac{K_{1_h}}{k_{2_h}} = V_1 + \int_o^\infty r_1(t) \, \mathrm{d}t, \tag{2.76}$$

where V is the total steady-state volume of distribution, and the impulse response function r_1 is defined as:

$$r_1(t) = \sum_{h=1}^{n-1} K_{1_h} \, \mathrm{e}^{-k_{2_h} t}. \tag{2.77}$$

The relaxation constants k_{2_h}, individually as well as collectively, have no simple biological meaning (see (2.43)). They are, in a sense, *descriptive* rather than *determinant* of the system. The relationship between the parameters of the impulse response function and the relaxation constants of each compartment must be worked out for each constellation of compartments. For the current example of at least four compartments in series, the relationship is worked out later.

Generalized Steady-State Solutions

Reversible Accumulation For $k_{2n-2} > 0$, the steady-state flux through the closed system is zero ($J_o = 0$), but the steady-state contents of the compartments are,

$$M_4 = \left(\frac{k_5}{k_6}\right) M_3 = \left(\frac{K_1 k_3 k_5}{k_2 k_4 k_6}\right) C_1,$$

$$M_3 = \left(\frac{K_1 k_3}{k_2 k_4}\right) C_1,$$

and

$$M_2 = \left(\frac{K_1}{k_2}\right) C_1$$

such that the sum of the magnitudes of the four compartments results in a chain of nested coefficient ratios,

$$\sum_{i=1}^{4} M_i = \left[V_1 + \frac{K_1}{k_2}\left(1 + \frac{k_3}{k_4}\left[1 + \frac{k_5}{k_6}\right]\right)\right] C_1 \tag{2.78}$$

which can be generalized to a closed system of n compartments in series,

$$\sum_{i=1}^{n} M_i = \left[V_1 + \frac{K_1}{k_2}\left(1 + \frac{k_3}{k_4}\left[1 + \frac{k_5}{k_6}\left(1 + \cdots + \left[1 + \frac{k_{2n-3}}{k_{2n-2}}\right]\right)\right]\right)\right] C_1, \tag{2.79}$$

where the last, or nth compartment, relative to the first compartment, has the size,

$$M_n = \left(\frac{K_1 k_3 k_5 \ldots k_{2n-3}}{k_2 k_4 k_6 \ldots k_{2n-2}}\right) C_1,$$

where n is the number of compartments. The generalization shows that a closed system maintains the steady-state content of one or more compartments at a level regulated by the relaxation constants of all preceding compartments in the series. For example, the last compartment may represent a neurotransmitter in the synaptic cleft.

The impulse response function yields the total content of the compartments in terms of its own relaxation constants according to (2.73),

$$\sum_{i=1}^{n} M_i = \left[V_1 + \sum_{h=1}^{n-1} \frac{K_{1_h}}{k_{2_h}}\right] C_1 \tag{2.80}$$

which yields the relationship between the individual compartmental relaxation constants and the powers of the exponentials of the impulse response function by the substitution of (2.79).

Irreversible Accumulation For $k_{2n-2} = 0$, the last compartment never reaches a steady-state. The compartment continues to expand while the preceding compartments eventually reach secular equilibria. The steady-state solution to this process is again the equation underlying the Gjedde–Patlak plot (see (2.53)),

$$\sum_{i=1}^{4} v_i(T) = V_1 + K\left(\frac{1}{k_3'} + \frac{1}{k_5}\right) + K\int_o^T \frac{c_1(t)}{C_1(T)}\mathrm{d}t, \tag{2.81}$$

where the apparent relaxation constant k_3' is,

$$k_3' = k_3\left(\frac{k_5}{k_4 + k_5}\right) \tag{2.82}$$

and

$$K = \frac{K_1}{1 + \frac{k_2}{k_3}\left(1 + \frac{k_4}{k_5}\right)} = \frac{K_1}{1 + \frac{k_2}{k_3'}} \tag{2.83}$$

which can be generalized to n compartments,

$$\sum_{i=1}^{n} v_i(T) = \left[V_1 + K\left(\frac{1}{k_3'} + \frac{1}{k_5'} + \frac{1}{k_7'} + \cdots + \frac{1}{k_{2i-1}'} + \cdots + \frac{1}{k_{2n-3}}\right)\right] + K\int_o^T \frac{c_1(t)}{C_1(T)}\mathrm{d}t, \tag{2.84}$$

where

$$k_{2i-1}' = \frac{k_{2i-1}}{1 + \frac{k_{2i-2}}{k_{2i-1}}\left[1 + \frac{k_{2i}}{k_{2i+1}}\left(1 + \cdots + \left[1 + \frac{k_{2n-4}}{k_{2n-3}}\right]\right)\right]} \tag{2.85}$$

and

$$K = \frac{K_1}{1 + \frac{k_2}{k_3}\left(1 + \frac{k_4}{k_5}\left[1 + \cdots + \left(1 + \frac{k_{2n-4}}{k_{2n-3}}\right)\right]\right)}. \tag{2.86}$$

The impulse response function defines the net clearance K in terms of the "unidirectional" clearance of the irreversibly accumulating compartment, $K_{1_{n-1}} = K$.

2.1.7 Multiple Compartments in Series and in Parallel

With a few exceptions (see Gunn et al. 2001), the impulse response function defines any constellation of linear compartmental systems, which can be described by first-order linear differential equations (Gunn et al. 2002), regardless of the structure.

Thus, also compartments in parallel follow the general principles underlying the steady-state solutions. The impulse-response function describes the constellation but its biological significance must be extracted from an analysis of the relationship between the relaxation constants of each compartment.

Generalized Steady-State Solution of Closed System of Branching Compartments

In a closed ("reversible") system as shown in Fig. 2.7, the steady-state flux through the system is of course zero ($J_o = 0$), but the solution to the steady-state magnitude of the combined compartments, generalized for any closed system of several parallel branches extending n steps from the origin, shows that parallel compartments are additive, while serial compartments are nested,

$$\sum_{i=1}^{\mathrm{n}} M_i = \left[V_1 + \frac{K_1}{k_2} \left(1 + \frac{k_{3_1}}{k_{4_1}} \left[1 + \frac{k_{5_{1_1}}}{k_{6_{1_1}}} + \cdots \right] + \frac{k_{3_2}}{k_{4_2}} \left[1 + \frac{k_{5_2}}{k_{6_2}} \left(1 + \cdots + \left[1 + \frac{k_{(2\mathrm{n}-3)_2}}{k_{(2\mathrm{n}-2)_2}} \right] \right) \right] \right) \right] C_1, \quad (2.87)$$

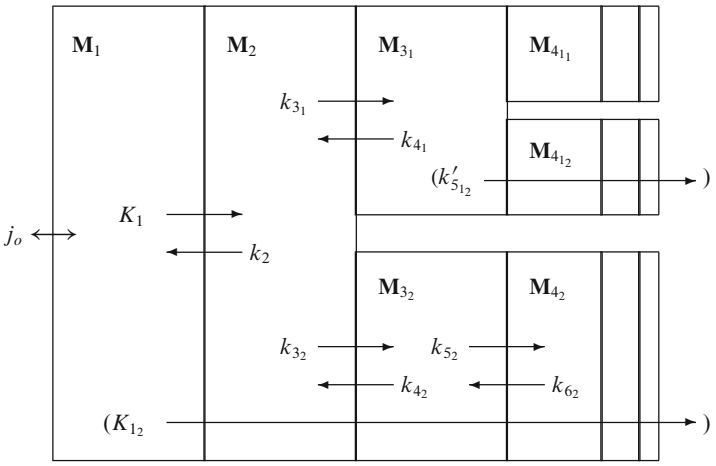

Fig. 2.7 Multiple compartments in series and parallel. Compartments in parallel are additive; compartments in series are nested. Branches 1_2 and 2 are open ("irreversible"), branch 1_1 is closed ("reversible"). Net clearances for open system are shown in brackets. Note that *apostrophes* ("primes") refer to composite rate constants or clearances which traverse several membranes

where the additional subscripts refer to the branch in question. The last compartment of the $n_{2\text{nd}}$ branch, relative to the first compartment, has the size

$$M_{n_2} = \left(\frac{K_1 \, k_{3_2} \, k_{5_2} ... k_{(2\text{n}-3)_2}}{k_2 \, k_{4_2} \, k_{6_2} ... k_{(2\text{n}-2)_2}} \right) C_1, \tag{2.88}$$

where n is the number of steps removed from the source. The generalization again shows that the closed system maintains the steady-state content of one or more compartments at a level that is regulated by the rate constants of the involved mechanisms. For example, the last compartment may represent a neurotransmitter and its level in the synaptic cleft.

Generalized Steady-State Solution of Open System of Branching Compartments

For an open system of n compartments in one branch ("2"), the net flux out of the branch is dictated by the net clearance to the sink of the branch,

$$K_{1_2} = \frac{K_1}{1 + \frac{k_2}{k_{3_2}} \left(1 + \frac{k_{4_2}}{k_{5_2}} \left[1 + \cdots + \left(1 + \frac{k_{(2\text{n}-2)_2}}{k_{(2\text{n}-1)_2}} \right) \right] \right)}, \tag{2.89}$$

where $K = K_{1_2}$ is the net clearance by branch 2 and n is the number of compartments leading to the sink governed by the rate constant $k_{2\text{n}-1_2}$. The corresponding magnitude of the nth compartment in this branch (open system) is given by:

$$M_{n_2} = \left(\frac{K_{1_2}}{k_{(2\text{n}-1)_2}} \right) C_1 \tag{2.90}$$

and the combined magnitude of all compartments (excluding the sink) in this open branch is

$$\sum_{i=1}^{n} M_{i_2} = \left[V_1 + K'_{1_2} \left(\frac{1}{k'_{3_2}} + \frac{1}{k'_{5_2}} + \frac{1}{k'_{7_2}} + \cdots + \frac{1}{k'_{(2i-1)_2}} + \cdots + \frac{1}{k_{(2n-1)_2}} \right) \right] C_1, \tag{2.91}$$

where

$$k'_{(2i-1)_2} = \frac{k_{(2i-1)_2}}{1 + \frac{k_{(2i)_2}}{k_{(2i+1)_2}} \left[1 + \frac{k_{(2i+2)_2}}{k_{(2i+3)_2}} \left(1 + \cdots + \left[1 + \frac{k_{(2n-2)_2}}{k_{(2n-1)_2}} \right] \right) \right]}, \tag{2.92}$$

where the apostrophe refers to the composite nature of the rate constant, which traverses multiple membranes.

2.2 Interpretation of Relaxation Constants

The biological reality is that concentrations vary in space but not normally in time. The compartmental kinetics must be translated from the space-invariant and time-variant model systems to the space-variant but time-invariant real pathways. Note that time-invariant (steady-state) variables, as earlier, are given as upper-case symbols.

In many cases, the relaxation constant k represents one of just a few processes, including flow, diffusion, membrane permeability, enzyme reaction, facilitated diffusion across membranes, or receptor binding. Depending on the processes known to establish the compartments occupied by a metabolite or by tracer molecules, relaxation constants can be estimated and interpreted in specific ways. In the case of tracer molecules, the molecules trace a specific set of processes, often because the tracer has been designed for the purpose of revealing the kinetics of just these processes.

2.2.1 Flow

When the flow of a solvent links two compartments, the relaxation of the downstream compartment $\mathbf{M_2}$ is due to the washout of the molecules dissolved in the effluent. This is an example of an open vascular system. The products $k_1 V_1$ and $k_2 V_2$ both equal the flow rate F, and k_2 equals the flow through the system per unit volume of the second compartment. Thus, the process establishes a proper compartment when F is constant,

$$k_2 = F/V_2 \tag{2.93}$$

as shown in Fig. 2.8.

The direct use of this model is limited to the dissolution of inert flow tracers in the bloodstream, which allow the estimation of flow rate, volume of distribution, and mean transit time ("bolus tracking") as in Ostergaard et al. (1998).

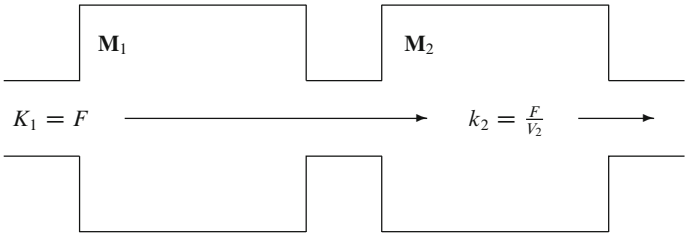

Fig. 2.8 Convection model of precursor and product compartments perfused by the solvent

2.2.2 Passive Diffusion

Diffusion is a fundamental process of elimination of concentration differences and release of entropy leading to a flux in the direction of a concentration gradient (see Chap. 1). In the unidirectional case, according to Fick's First Law, the one-dimensional flux is given by (Gjedde 1995a),

$$J = -\mathrm{DA}\,\frac{\mathrm{d}C}{\mathrm{d}x}, \tag{2.94}$$

where D is the diffusion coefficient, A the cross-sectional area of the volume through which the unidirectional diffusion occurs, and $\mathrm{d}C/dx$ is the *gradient* (G), equal to the slope of the concentration (or activity) curve or plane at the coordinate x. In a closed system, the concentration gradient is eventually dissipated until $J = 0$ when $\mathrm{d}C/dx = 0$. The system is at *equilibrium* when net flux is no longer taking place and $\mathrm{d}C/\mathrm{d}t$ reaches zero. If the diffusing substance undergoes no change other than the diffusion itself, the temporal rate of elimination of the concentration gradient is proportional to the spatially negative rate of change of the gradient,

$$\frac{\partial c}{\partial t} = -D\,\frac{\mathrm{d}G}{\mathrm{d}x}, \tag{2.95}$$

where G is the gradient, such that,

$$\frac{\partial c}{\partial t} = -D\,\frac{\partial^2 c}{\partial x^2}, \tag{2.96}$$

where the diffusion coefficient is the proportionality factor. Thus, when the substance is uniformly distributed in the volume, diffusion ceases. In this sense, passive diffusion and compartmentation are mutually incompatible concepts, as compartments have no internal concentration gradients because the gradients are placed at two-dimensional interfaces between the compartments.

The purpose of the treatment below is to establish the extent to which varying concentration profiles within compartments are consistent with compartmental kinetics, i.e., the extent to which a diffusion process can be given a pseudo-compartmental description which satisfies the criteria of compartment kinetics. The task becomes one of the determination of the concentration profiles and total contents of substance which different structural arrangements give rise to, while maintaining the steady-state of the concentration of the diffusing substances.

Steady-State One-Dimensional Diffusion

In the simplest steady-state condition the rate of change of the diffusing substance with respect to time is nil ($\partial c_1/\partial t = 0$) but the rate of change of the diffusing substance with respect to distance (one-dimensional space) is significant

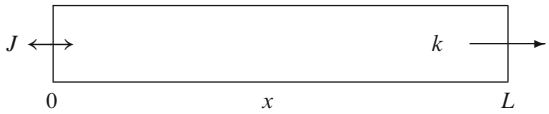

Fig. 2.9 Single compartment with simple passive one-dimensional diffusion due to Brownian motion

($\partial C_1/\partial x \neq 0$). This condition can be evaluated by application of the diffusion equation to the case of one-dimensional diffusion in one direction (x) through a volume ("box") in which no concentration gradients exist in the orthogonal directions y and z, and substance is lost or gained only at the ends of the box as shown in Fig. 2.9.

When the concentration of the substance is kept constant, the spatial rate of change of the gradient is nil,

$$\frac{\mathrm{d}^2 C}{\mathrm{d}x^2} = 0 \tag{2.97}$$

and the result is a constant (or uniform) gradient,

$$G(x) = \frac{\mathrm{d}C}{\mathrm{d}x} = \alpha \tag{2.98}$$

with a linearly stationary concentration profile,

$$C(x) = \alpha\, x + C(0) \tag{2.99}$$

with a slope of the magnitude α,

$$\alpha = \frac{C(x) - C(0)}{x} \tag{2.100}$$

and a steady-state flux for a box of length $x = L$ of,

$$J_o = -\mathrm{DA}\,\frac{C(L) - C(0)}{L} = -\mathrm{DA}\,\frac{\Delta C}{L} \tag{2.101}$$

as well as a steady-state content of the "box" of,

$$M = L\, A\, \frac{C(L) + C(0)}{2} = L\, A\, \overline{C}, \tag{2.102}$$

where $\overline{C}$ is the average steady-state concentration of the compartment. Then, the effective relaxation constant of the efflux is

$$k = \frac{J}{M} = -\left(\frac{D\, \Delta C}{L^2\, \overline{C}}\right), \tag{2.103}$$

where $L^2/(2D) = \tau_D$ is the characteristic time constant of diffusion along the distance L obtained from the equation derived by Einstein (1908), such that

$$k = -\left(\frac{\Delta C}{2\,\tau_D\,\overline{C}}\right), \tag{2.104}$$

where the relaxation constant of the substance undergoing passive diffusion is the inverse of the time constant of diffusion if the concentration $C(0)$ is kept constant by quantitative removal to the external medium. From the opposite perspective, the product of k and τ_D can be said to determine the difference between the concentrations at the two extremes of the diffusion path,

$$\Delta C = -2\,k\,\tau_D\,\overline{C}, \tag{2.105}$$

where τ_D is proportional to the square of the length of the diffusion path. Thus, a large concentration difference is favored by long diffusion paths and, conversely, a small or negligible concentration difference is favored by very short diffusion paths, once the relaxation constant of the compartment is given.

Steady-State Passive Diffusion with Concentration-Dependent Loss

Unless the external concentrations are kept constant, equilibrium will eventually ensue. Equilibrium is anathema to the biological *steady-state* in which $dC_1/dt = 0$ because the gradient is preserved by energy-requiring processes which maintain the flux by establishing constant concentrations at both ends of the diffusion path. Alternatively, substance may be removed continuously from the diffusion path by a concentration dependent process occurring in the directions orthogonal to the direction of passive diffusion (x) as shown in Fig. 2.10. If the volume is sufficiently narrow in the orthogonal directions (infinitely long narrow tube with a cross-sectional area of A), and the product of the rate constant of removal and the time constant of diffusion is very small, no concentration gradients exist in the orthogonal directions.

The spatial rate of change of the gradient is now a function of the rate of removal of the substance along the length of the tube,

$$\frac{d^2C}{dx^2} = \left(\frac{k}{D}\right)C(x), \tag{2.106}$$

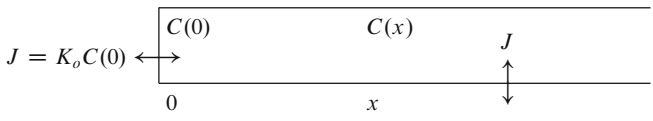

Fig. 2.10 Single compartment with simple passive one-dimensional diffusion through infinitely long tube with concentration-dependent loss

where x is the distance along the length of the tube and k is the relaxation constant of a concentration-dependent loss in the orthogonal y and z directions. At steady-state, the gradient is the monoexponential function satisfying (2.106),

$$G(x) = \frac{\mathrm{d}C}{\mathrm{d}x} = -C(0)\,\mathrm{e}^{-x\sqrt{k/D}}\,\sqrt{k/D} \tag{2.107}$$

with the concentration profile,

$$C(x) = C(0)\,\mathrm{e}^{-x\sqrt{k/D}} \tag{2.108}$$

as well as the total content of the infinitely long tube,

$$M = A\int_o^\infty C(x)\,\mathrm{d}x = A\,C(0)\,\sqrt{D/k}, \tag{2.109}$$

where M is the steady-state content of the infinitely long tube in which the concentration declines to zero. The constant $\sqrt{D/k}$ is a characteristic length constant, l_D, which depends only on the system. The constant $\sqrt{k/D}$ is therefore the inverse length constant, and the constant $\sqrt{Dk}$ is the ratio between the length constant and the time constant of diffusion, $l_\mathrm{D}/\tau_\mathrm{D}$. The entire loss of substance therefore occurs in the orthogonal directions, i.e., through the wall of the tube. The efflux through the wall of this virtual compartment is given by:

$$J = k\,A\int_o^\infty C(x)\,\mathrm{d}x = A\,C(0)\,\sqrt{Dk} \tag{2.110}$$

which confirms that k is indeed the steady-state relaxation constant of the compartment,

$$k = \frac{J}{M} = D\left(\frac{A\,C(0)}{M}\right)^2, \tag{2.111}$$

where the term $M/[A\;C(0)]$ reveals that the characteristic length constant l_D in reality is the diffusion distance effectively reached in the tube. As the compartment is in steady-state and no substance is lost or gained at the end of the tube, the flux into the origin of the tube must be of the same magnitude as the flux through the wall. The influx is determined by the value of the gradient at $x = 0$,

$$J = -D\;A\;G(0) = A\,C(0)\,\sqrt{Dk} \tag{2.112}$$

such that (2.108) becomes also,

$$C(x) = C(0)\,\mathrm{e}^{-x\;kA\;C(0)/J} \tag{2.113}$$

in which the spatial rate constant of the monoexponential decline is a function of the rate constant of loss or gain through the wall of the tube and the apparent clearance

of substance by diffusion into the tube. We now define a clearance as the volume of the precursor compartment which per unit time is cleared of the substance by the diffusion into the infinitely long tube,

$$C(x) = C(0)\, \mathrm{e}^{-x\, kA/K_o}, \tag{2.114}$$

where K_o is a characteristic clearance of substance into the tube, equal to $A\sqrt{Dk}$ or $A\ l_{\mathrm{D}}/\tau_{\mathrm{D}}$. As the ratio $J/C(0)$, this clearance depends only on the properties of the system that include the cross-sectional area and the length and time constants of the tube (Fig. 2.10).

Steady-State Diffusion with Concentration-Dependent Loss and Backflux

Substance can also be added to the diffusion path by a concentration-independent transfer in the directions orthogonal to the direction of passive diffusion. Such a process could be a second compartment continuously feeding the diffusion path, as shown in Fig. 2.11.

The spatial rate of change of the gradient is now a function of the net removal or addition of substance along the length of the tube,

$$\frac{\mathrm{d}^2 C_1}{\mathrm{d}x^2} = \left(\frac{k}{D}\right)[C_1(x) - C_2], \tag{2.115}$$

where x is the distance along the length of the tube, k the relaxation constant of the concentration-dependent loss, and kC_2 is the constant rate of gain by flux into the diffusion path, when the concentration C_2 is kept constant by the flux J_2. The general solution to (2.115) is given by:

$$C_1(x) = C_2 + \alpha \mathrm{e}^{-(L-x)\sqrt{k/D}} + \beta \mathrm{e}^{-(L-x)\sqrt{k/D}}$$

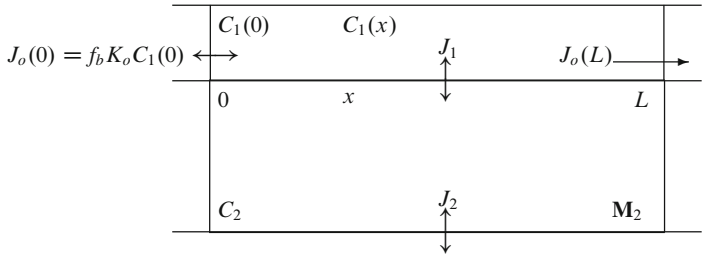

Fig. 2.11 System of two compartments with simple passive one-dimensional diffusion through tube of finite length with concentration dependent loss to, and concentration independent gain from, the surrounding mantle compartment

as can easily be verified by substitution. The constants of integration, α and β, are determined by boundary conditions. The constants may be written in terms of the boundary values, $C_1(0)$ and $C_1(L)$, as follows:

$$\alpha = \frac{e^{L\sqrt{k/D}}[C_1(0) - C_2] - [C_1(L) - C_2]}{e^{L\sqrt{k/D}} - e^{-L\sqrt{k/D}}}$$

and

$$\beta = \frac{e^{L\sqrt{k/D}}[C_1(L) - C_2] - [C_1(0) - C_2]}{e^{L\sqrt{k/D}} - e^{-L\sqrt{k/D}}}.$$

In cases such as that of non-synaptic transmission, where diffusion is over relatively long distances, $C_1(x)$ tends to decay exponentially, as if $\beta \approx 0$. This will be the case if $L\sqrt{k/D}$ is relatively large and the ratio $[C_1(L) - C_2]/[C_1(0) - C_2]$ is relatively small. Making that assumption,

$$C_1(x) \approx C_2 + [C_1(0) - C_2]e^{-x\sqrt{k/D}},$$

which is essentially (2.117), below. At steady-state, the gradient is given by the appropriate boundary conditions,

$$G(x) = \frac{dC_1}{dx} = \sqrt{k/D}\ [C_2 - C_1(0)]\ e^{-x\sqrt{k/D}}, \tag{2.116}$$

where $\sqrt{k/D}$ is the inverse length constant $(1/l)$. The equation yields the concentration profile when integrated,

$$C_1(x) = C_2 + (C_1(0) - C_2)\, e^{-x\sqrt{k/D}} \tag{2.117}$$

that approaches C_2 rather than the zero of the previous condition. The backflux reduces the gradient of the substance in the tube and, hence, reduces the clearance of substance into the origin of the tube. The influx of substance at the origin of the tube can be evaluated from the gradient at $x = 0$,

$$J_o(0) = -D\ A\ G(0) = A\ \sqrt{Dk}\ (C_1(0) - C_2) \tag{2.118}$$

which relates the influx to the concentration of the diffusing substance at the entrance and to the net gain or loss of substance by transfer in the direction orthogonal to the diffusion path. Let the clearance of substance into the diffusion path from the external source be reduced by backflux to the real clearance by diffusion, K'_o, from the previously defined maximum clearance K_o in the absence of backflux from the compartment $\mathbf{M_2}$ to the tube,

$$K'_o \equiv \frac{J_o(0)}{C_1(0)} = A\sqrt{Dk}\ \left(1 - \frac{C_2}{C_1(0)}\right) = f_b\ A\sqrt{Dk} = f_b\ K_o, \tag{2.119}$$

where the fraction f_b, equal to $1 - [C_2/C_1(0)]$, depends on the concentration difference at the entrance to the tube. The term f_b is a key factor in the remaining

treatment. The fraction f_b accounts for the reduction of the clearance ("backflux") by the bidirectional transfer, such that the influx is,

$$J_o(0) = f_b\ K_o\ C_1(0) = K'_o\ C_1(0) \tag{2.120}$$

for which the concentration profile along the diffusion path is,

$$C_1(x) = C_1(0)\left[1 - f_b\left(1 - \mathrm{e}^{-x f_b k A / K'_o}\right)\right] \tag{2.121}$$

and the flux of substance at $x = L$ likewise becomes,

$$J_o(L) + J_1(L) = -\mathrm{DA}\ G(L) = A\sqrt{Dk}\ \ (C_1(0) - C_2)\ \ \mathrm{e}^{-L\sqrt{k/D}}$$

of which the efflux is,

$$J_o(L) = K'_o\ C_1(L)\ = K'_o\ C_1(0)\left[1 - f_b\left(1 - \mathrm{e}^{-f_b k L A / K'_o}\right)\right], \tag{2.122}$$

where the product LA is the volume of the tubular diffusion path. The net flux in the directions orthogonal to the diffusion path can now be calculated as the difference,

$$J_1 = J_o(0) - J_o(L) = f_b\ K'_o\ C_1(0)\ \left(1 - \mathrm{e}^{-f_b k L A / K'_o}\right) \tag{2.123}$$

which is zero when f_b is zero.[1]

2.2.3 *Properties of Delivery Compartment*

Diffusion-Limited Membrane Permeability

Membrane permeability is a special case of passive diffusion without loss or gain in which the dimensions are fixed but the concentrations on the two sides of the membrane may vary. In this treatment, the membrane is the lining of the narrow tube discussed earlier (Fig. 2.12).

[1] The solution is not defined for k equal to zero, because the gradient expressed in (2.116) then has the simpler solution,

$$G(x) = \frac{\mathrm{d}C}{\mathrm{d}x} = \frac{I}{D}\ x + H_1, \tag{2.124}$$

where $C_2 \neq I/k$, which yields the concentration profile,

$$C(x) = \frac{I}{2D}\ x^2 + H_1 x + H_2, \tag{2.125}$$

where H_1 and H_2 depend on the conditions. This formula can be applied to the concentration independent consumption of oxygen diffusing unidirectionally through a tissue.

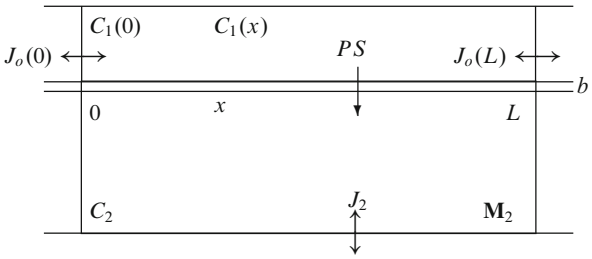

Fig. 2.12 Two compartments separated by membrane with diffusion-limited permeability through wall of thickness b of tube of finite length L

The diffusion flux is described by (2.101), modified to include the concentrations of the diffusing substance in the medium surrounding the membrane, rather than in the membrane itself,

$$\mathrm{d}J = -D'\mathrm{d}S\,\frac{C_1(x,b) - C_1(x,0)}{b} = -D'\mathrm{d}S\,\frac{\Delta C_1}{b}, \tag{2.126}$$

where b is the width of the membrane. The ratio D'/b is defined as the permeability coefficient P, the prime referring to the possibly different solubilities of the diffusing substance in the membrane and the surrounding media, and S is defined as the surface area of the membrane to distinguish that area from A, the cross-sectional area of the tube. Thus,

$$\mathrm{d}J = -P\mathrm{d}S\;\Delta C_1, \tag{2.127}$$

where $P\mathrm{d}S$ (as a clearance) has unit of flow. Let a tube of length L and inner volume $V_1 = AL$ be lined by a membrane of thickness b and surface area S for which $C_1(x,b) = C_2$ for all x. The relaxation constant of the efflux through the membrane is then given by (2.93),

$$k = P\;\mathrm{d}S/\mathrm{d}V_1 = PS/V_1 \tag{2.128}$$

such that (2.121) together yield the concentration profile along the length of the tube,

$$C_1(x) = C_1(0)\left[1 - f_b\left(1 - \mathrm{e}^{-f_b\;(x/L)(PS/K'_o)}\right)\right], \tag{2.129}$$

where $LA = V_1$, the volume of the entire length of the tube. The relation expresses the monoexponential decline of the concentration along the length of the tube when diffusion in the tube is accompanied by permeation of the membrane lining the tube. For $x = L$, the concentration declines to the expression,

$$C_1(L) = C_1(0)\left[1 - f_b\left(1 - \mathrm{e}^{-f_b\;PS/K'_o}\right)\right], \tag{2.130}$$

where, as earlier, $K'_o = f_b\ A\sqrt{Dk} = f_b\ \sqrt{DAPS/L}$, such that,

$$C_1(L) = C_1(0)\left[1 - f_b\left(1 - \mathrm{e}^{-\sqrt{PSL/(\mathrm{DA})}}\right)\right] = C_1(0)\left[1 - f_b\left(1 - \mathrm{e}^{-L\sqrt{2P/(Dr)}}\right)\right], \tag{2.131}$$

where P is the permeability of the membrane, D the diffusion coefficient of the substance diffusing through the tube, and r is the radius of the tube. It turns out that this expression can be generalized also to the case of convection through the tube in which the clearance into the proximal end of the tube, and hence the diffusion, is replaced by convection.

When the tube is of finite length, the relaxation constant of the compartment formed by the tube no longer equals just PS/V_1. The content of the compartment is,

$$\begin{aligned} M_1(L) &= A\int_o^L C_1(0)\left(1 - f_b\left[1 - \mathrm{e}^{-\frac{xf_bPS}{LK'_o}}\right]\right)\mathrm{d}x \\ &= V_1 C_1(0)\left[1 - f_b\left(1 - \frac{1 - \mathrm{e}^{-f_bPS/K'_o}}{f_bPS/K'_o}\right)\right] \end{aligned} \tag{2.132}$$

where $M_1(L)$ is the total mass of the substance in the tube of finite length L in which the concentration declines to $C_1(L)$. The decay of the compartment, therefore, occurs both through the wall and at the end of the tube. The net flux across the wall of the tube is given by:

$$J_1 = \frac{PSA}{V_1}\int_o^L (C_1(x) - C_2)\ \mathrm{d}x = f_b\ K'_o\ C_1(0)\ \left(1 - \mathrm{e}^{-f_bPS/K'_o}\right) \tag{2.133}$$

while the efflux from the end of the tube is given by:

$$J_o(L) = K'_o\ C_1(0)\ \left[1 - f_b\ \left(1 - \mathrm{e}^{-f_bPS/K'_o}\right)\right] \tag{2.134}$$

such that the total flux, equal to the flux at the entry, is,

$$J_o(0) = J_1 + J_o(L) = K'_o\ C_1(0) \tag{2.135}$$

which yields the true relaxation constant of the entire contents of the compartment formed by the tube of finite length,

$$\begin{aligned} k_o = \frac{J_o(0)}{M_1(L)} &= \left[\frac{K'_o}{V_1}\right]\left(\frac{PS}{PS(1 - f_b) + K'_o\ (1 - \mathrm{e}^{-f_bPS/K'_o})}\right) \\ &= \frac{PS/V_1}{1 - \mathrm{e}^{-PS/K_o}}\ \text{for}\ f_b = 1 \end{aligned} \tag{2.136}$$

which approaches either K'_o/V_1 when the PS product is small relative to the magnitude of the clearance (observe the equivalence with (2.93)) or PS/V_1 when the PS

product is large relative to K'_o and f_b is unity ($K'_o = K_o$, no gain by influx from compartment $\mathbf{M_2}$). The effective relaxation constant of the loss to compartment $\mathbf{M_2}$ is,

$$k_1 = \frac{J_1}{M_1} \tag{2.137}$$

such that

$$k_1 = \left[\frac{K'_o}{V_1}\right]\left(\frac{1 - e^{-f_b PS/K'_o}}{1 - f_b\left(1 - \frac{1-e^{-f_b PS/K'_o}}{f_b PS/K'_o}\right)}\right) = \left[\frac{K'_o}{V_o}\right]\left(1 - e^{-f_b PS/K'_o}\right), \tag{2.138}$$

where V_o is an apparent volume defined as $M_1/C_1(0)$, which expresses the relaxation of the diffusion path in terms of a virtual compartment with a uniform concentration equal to $C_1(0)$. This convention converts the diffusion path to a virtual compartment, which conforms to the fundamental definition.

Flow-Limited Membrane Permeability

Flow-limited membrane permeability is a special case of flow-dependent exchange between two compartments when solvent flows through the precursor compartment, and a fixed fraction of the solvent is cleared of the solute by permeation of the solute into the second compartment. The two compartments are separated by a membrane which is impermeable to the solvent but not to the solute (semipermeable membrane). A typical example of this system is the capillary with its surrounding tissue mantle.

The exchange of substance between the capillary and the tissue is assumed to be nonenergy-requiring (passive) and, thus, to proceed only in the direction of the solute concentration difference between the two compartments. The system is considered to be closed if the solute in the product compartment decays exclusively by return to the precursor compartment.

As described earlier, the contents of the capillary bed do not reside in a true compartment, because the relaxation constant for the flux through the wall, by means of which a fraction of the solute ($E = J_1/J_o(0)$) enters the exchange compartment, equals $k_1 = K'_o\left(1 - e^{-f_b PS/K'_o}\right)/V_o$ rather than PS/V_1. Nonetheless, as derived earlier (2.138), it is possible to reduce the capillary to the status of a compartment by showing when it decays as required of a compartment.

The clearance of a fraction of the contents of the delivery compartment to the exchange compartment is a function both of the permeability-surface area product of the membrane through which the transfer occurs and the flow of the solvent in the tube lined by this membrane, as derived by Crone (1963). Crone derived the clearance on the condition that no more than a negligible amount of capillary solute actually accumulate in the tissue compartment (i.e., when $C_1(x, b) = 0$ for all x), for example because the tissue volume of distribution is very large, or because the solute is quantitatively consumed in the tissue. In this condition, $f_b = 1$, where $1 - f_b$ is the concentration ratio between tissue and capillary at the site of arterial entry.

The clearance equations can be derived for the bidirectional case, in which f_b is less than unity. The flow of a solute through the delivery compartment, combined with the transaxial loss of solute to the surrounding mantle, can be represented by an apparent diffusion coefficient. Let the delivery compartment be a narrow tube of length L, cross-sectional area A, volume V_1, wall permeability-surface area PS, and flow F. The flow term F replaces the term for the clearance as reduced by backflux (K_o'). The apparent diffusion coefficient of the solute is then the solution to (2.119) where F replaces K_o',

$$D_{\text{app}} = \left(\frac{F}{f_b A}\right)^2 \frac{V_1}{PS}, \tag{2.139}$$

where, again, f_b is the bidirectionality fraction which reduces the effective clearance by the backflux. The fundamental flux equation for the loss of solute at any distance along the capillary then is given by an expression, which is formally analogous to the diffusion equation,

$$J_1 = -D_{\text{app}} A \frac{\mathrm{d}C_1}{\mathrm{d}x} = -\left(\frac{F}{f_b}\right)^2 \left[\frac{V_1}{A\,PS}\right] \frac{\mathrm{d}C_1}{\mathrm{d}x} \tag{2.140}$$

where the spatial rate of change of the solute gradient in the delivery compartment at steady-state is given by,

$$\frac{\mathrm{d}^2 C_1}{\mathrm{d}x^2} = \left(\frac{f_b PS}{\mathrm{FL}}\right)^2 (C_1(x) - C_2) = \left(\frac{f_b PS}{\mathrm{FL}}\right)^2 (C_1(x) - [1 - f_b]\, C_1(0)) \tag{2.141}$$

such that the gradient is,

$$\frac{\mathrm{d}C_1}{\mathrm{d}x} = \left(\frac{f_b PS}{\mathrm{FL}}\right) \left[(f_b - 1)\, C_1(0) \; - f_b\, C_1(0)\, \mathrm{e}^{-x f_b PS/(\mathrm{FL})}\right] \tag{2.142}$$

and the concentration profile of the solute in the delivery compartment as before is,

$$C_1(x) = C_1(0) \left(1 - f_b \left[1 - \mathrm{e}^{-x f_b PS/(\mathrm{FL})}\right]\right). \tag{2.143}$$

Capillary Model of Bidirectional Flux

In the living organism, the delivery compartment usually (but not always) is a capillary. In those cases, replace $C_1(0)$ by C_a, the symbol of the arterial concentration, x by L, and $C_1(L)$ by C_v, the symbol of the venous concentration. The fundamental equations of the capillary exchange then emerge from (2.143) as:

$$C_v = C_\mathrm{a} \left[1 - f_b \left(1 - \mathrm{e}^{-f_b PS/F}\right)\right] \tag{2.144}$$

in which the net flux across the capillary wall is given by (2.123) and (2.133) for $C_1(0) = C_a$ and $K'_o = F$,

$$J_1 = f_b\, C_a\, F \left(1 - e^{-f_b PS/F}\right) \tag{2.145}$$

and

$$J_o(0) = F\, C_a \tag{2.146}$$

whence the extraction fraction associated with this unidirectional transfer arises as the ratio between the flux into the capillary and the efflux through the wall,

$$E = 1 - \frac{C_v}{C_a} = \frac{J_1}{J_o(0)} = f_b \left(1 - e^{-f_b PS/F}\right) \tag{2.147}$$

which defines the steady-state extraction fraction. Only in the case of zero tissue concentration, i.e., $f_b = 1$, does this equation reduce to the relationship derived by Crone (1963),

$$E_o = 1 - e^{-PS/F} \tag{2.148}$$

which thus is valid only for substances of sufficiently low permeability. The total actual content of the capillary compartment is given by (2.132),

$$M_1 = V_1\, C_a \left[1 - f_b \left(1 - \frac{1 - e^{-f_b PS/F}}{f_b PS/F}\right)\right] = V_o C_a \tag{2.149}$$

in which V_o defines a virtual volume of the delivery compartment with the uniform concentration C_a. The virtual delivery compartment represents the redistribution of M_1 in a volume, V_o, so small that the concentration uniformly is $C_1(0)$. The redistribution shows that M_1 fulfills the criteria of a compartment with a volume of V_o

$$V_o = V_1 \left[1 - f_b \left(1 - \frac{1 - e^{-f_b PS/F}}{f_b PS/F}\right)\right], \tag{2.150}$$

where the real average concentration in the physical volume V_1 is,

$$\overline{C}_1 = C_a \left[1 - f_b \left(1 - \frac{1 - e^{-f_b PS/F}}{f_b PS/F}\right)\right] \tag{2.151}$$

such that the "virtual" and the real compartments have the same contents but different apparent volumes.

In the case of bidirectional transfer, f_b is less than unity. The simplest way to describe the transfer in terms of compartmental kinetics is to split the net flux into efflux and influx, as shown by (2.135) and (2.145), such that

$$J_1 = C_a\, F\, E_o, \tag{2.152}$$

where K_1 is an apparent clearance, also known as the Capillary Diffusion Capacity, in the direction of transfer from delivery compartment to exchange compartment. It is also the ratio between a fictive unidirectional flux through the wall of the capillary and the arterial concentration, obtained by setting $f_b = 1$,

$$K_1 = F\left(1 - \mathrm{e}^{-PS/F}\right) = F\ E_o \tag{2.153}$$

such that the same fictive unidirectional flux is given by:

$$\overrightarrow{J_1} = f_b K_1\ C_\mathrm{a}, \tag{2.154}$$

where the relaxation constant k_1 for this fictive unidirectional flux is,

$$k_1 = \frac{\overrightarrow{J_1}}{M_1} = F\left(1 - \mathrm{e}^{-PS/F}\right)/V_o = K_1/V_o. \tag{2.155}$$

The fictive unidirectional flux in the opposite direction is then,

$$\overleftarrow{J_1} = J_1 - \overrightarrow{J_1} = (1 - f_b)\ C_\mathrm{a}\ K_1 \tag{2.156}$$

with the relaxation constant given by the fractional clearance,

$$k_2 = \frac{\overleftarrow{J_1}}{M_2} = \frac{F}{V_2}\left(1 - \mathrm{e}^{-PS/F}\right) = K_1/V_2, \tag{2.157}$$

where M_2 equals $(1 - f_b)\ C_\mathrm{a}\ V_2$, indicating that the compartment exists when the flow, volume, and permeability-surface area terms are at steady-state, as shown in the model of Fig. 2.13.

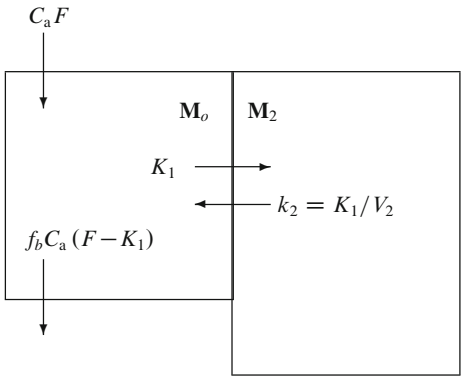

Fig. 2.13 Compartmental model of capillary and tissue compartments in which the tissue compartment clears precursor from solvent flowing through the capillary compartment by means of semi-permeable membrane. $\mathbf{M}_0$ is a virtual compartment with the smaller (virtual) volume V_o, uniform concentration $C_\mathrm{a} = C_1(0)$, and a substance content of M_1. The fraction $1 - f_b$ is the ratio between concentrations of solute in tissue and capillary compartments

Very large values of the *PS* term relative to F turn the clearance compartment into a flow-limited compartment in which the magnitude of the flow determines the influx to the compartment. On the other hand, very low values of the *PS* product relative to F turn the compartment into a diffusion-limited compartment in which the magnitude of the permeability determines the influx to the product compartment. The ratio between the parameters K_1 and K_1/V_2 is the volume of the solvent V_2 in the product compartment.

Thus, depending on the magnitude of the *PS* product, the rate constant is an index either of the flow through the system, relative to its volume, or of the permeability-surface area product of the interface, also relative to the volume of the system.

2.2.4 Protein–Ligand Interaction

In their simplest form, the three processes of enzyme reaction, facilitated diffusion across membranes, and receptor binding are variations on the same underlying theme. The theme received its steady-state formulation by Briggs and Haldane (1925), as an extension of the original equilibrium solution of Michaelis and Menten (1913). The key mechanism is the binding of a ligand to sites on the protein. The interacting compartment $\mathbf{M_2}$ is normally either open when it acts as a catalyst or transporter, or closed when it predominantly acts as a receptor (Fig. 2.14).

Competitive Interaction

The protein releases the bound ligand (m_2) at a constant rate to the same or a different compartment, either as the intact precursor (m_1) or as a transformed or translocated product (m_3), thus freeing the protein for new occupation, according to the general formula,

$$\frac{\mathrm{d}m_2}{\mathrm{d}t} = (j_1 + j_2) - (k_2 + k_3)\, m_2. \tag{2.158}$$

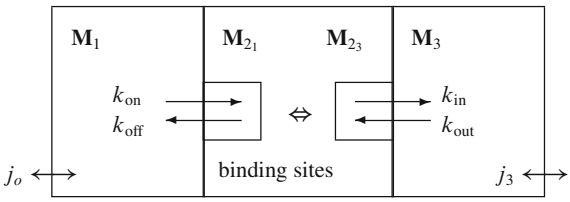

Fig. 2.14 Model of protein–ligand interaction. Unbound ligands (m_1 and m_3) in respective compartments ($\mathbf{M}_1$ and $\mathbf{M}_3$) interact with sites on protein ($\mathbf{M}_{2_1}$ and $\mathbf{M}_{2_3}$). Maximum number of available sites is $B_{\max}$

The size of the protein compartment is a function of the magnitude of these coefficients, some of which combine to define the interaction of the protein with two or more competitors for the same sites,

$$\frac{\mathrm{d}m_2}{\mathrm{d}t} = \left[\frac{k_{\text{on}}\,(B_{\max} - m_2)}{V_1}\right] m_1 + \left[\frac{k_{\text{out}}\,(B_{\max} - m_2)}{V_3}\right] m_3 - (k_{\text{off}} + k_{\text{in}})\, m_2, \tag{2.159}$$

where m_1 and m_3 are the masses of competitors in compartments $\mathbf{M}_1$ and $\mathbf{M}_3$, and m_2 is the sum of the competitors attached to the binding sites. Equation (2.159) is usually rearranged to allow an evaluation of whether $\mathbf{M}_2$ has the characteristics of a compartment.

Combination of the variables of (2.159) from this perspective yields an equation with m_2 as the independent variable,

$$\begin{aligned}\frac{\mathrm{d}m_2}{\mathrm{d}t} = {} & \left[\frac{k_{\text{on}}\, B_{\max}}{V_1}\right] m_1 + \left[\frac{k_{\text{out}}\, B_{\max}}{V_3}\right] m_3 - (k_{\text{off}} + k_{\text{in}})\, m_2 \\ & -(k_{\text{off}} + k_{\text{in}}) \left(\left[\frac{k_{\text{on}}}{k_{\text{off}} + k_{\text{in}}}\right]\left[\frac{m_1\, m_2}{V_1}\right] + \left[\frac{k_{\text{out}}}{k_{\text{off}} + k_{\text{in}}}\right]\left[\frac{m_3\, m_2}{V_3}\right] \right)\end{aligned} \tag{2.160}$$

which shows that the bound ligand constitutes a simple compartment only when m_1 and m_3 remain constant (or effectively nil). The terms $(k_{\text{off}} + k_{\text{in}})/k_{\text{on}}$ and $(k_{\text{off}} + k_{\text{in}})/k_{\text{out}}$ define the Michaelis half-saturation concentrations K_{M_1} and K_{M_3}, and the terms $k_{\text{off}}/k_{\text{on}}$ and $k_{\text{in}}/k_{\text{out}}$ the dissociation constants K_{d_1} and K_{d_3}, e.g.,

$$K_{\text{M}_1} = \frac{k_{\text{off}} + k_{\text{in}}}{k_{\text{on}}} = K_{d_1} + \frac{k_{\text{in}}}{k_{\text{on}}} \tag{2.161}$$

which in turn shows that K_{M} is always greater than K_d when there is significant translocation of substrate.

Competitive Inhibition For the steady-state of $\mathrm{d}m_2/\mathrm{d}t = 0$, (2.160) yields the famous Michaelis–Menten equation for competition between two ligands (Dixon 1953),

$$M_2 = B_{\max}\left[\frac{C_1}{K_{\text{M}_1}\left(1 + \frac{C_3}{K_{\text{M}_3}}\right) + C_1} + \frac{C_3}{K_{\text{M}_3}\left(1 + \frac{C_1}{K_{\text{M}_1}}\right) + C_3}\right], \tag{2.162}$$

where $C_1 = M_1/V_1$ and $C_3 = M_3/V_3$. The ratio $M_2/B_{\max}$ is the combined occupancies (σ) of the ligands,

$$\sum \sigma = \frac{\frac{C_1}{K_{\text{M}_1}} + \frac{C_3}{K_{\text{M}_3}}}{1 + \frac{C_1}{K_{\text{M}_1}} + \frac{C_3}{K_{\text{M}_3}}} = \frac{\chi_1 + \chi_3}{1 + \chi_1 + \chi_3} = \frac{\sum \chi}{1 + \sum \chi}, \tag{2.163}$$

where χ_1 is the ratio C_1/K_{M_1}, the normalized or relative concentration of the ligand in the precursor compartment, and χ_3 is the ratio C_3/K_{M_3}. The occupancy of ligand m_1 is then,

$$\sigma_1 = \frac{\chi_1}{1 + \sum \chi} \tag{2.164}$$

which expresses the effect of the competition between the two ligands when the occupation by one ligand causes the occupancy of other ligands to decline.

The bound ligand relative to the unbound ligand at steady-state can be expressed as a binding potential, obtained from (2.162), as in Gjedde et al. (1986),

$$p_{B_1}(\chi_1) = \frac{M_{2_1}}{M_1} = \frac{\sigma_1 \; B_{max}}{M_1} = \frac{B_{max}}{V_1 \; K_{M_1} \; (1 + \sum \chi)} = \frac{p_{B_1}(0)}{1 + \sum \chi}, \tag{2.165}$$

where p_B is a binding potential, the change of which reflects any change of B_{max}, C_1, or C_2. This equation linearizes to the Eadie–Hofstee equation (Eadie 1952),

$$M_{2_1} = B_{max} - [V_1 \; K_{M_1} \; (1 + \chi_3)] \; p_{B_1}(\chi_1) \tag{2.166}$$

according to which competitive interaction increases the magnitude of the Michaelis constant in proportion to the magnitude of competitor concentrations, χ_3, provided they are constant.

Depending on its function, the protein exerts its function when it unites with the occupant, either by reacting with other molecules or by translocating the product to another compartment. If the translocated product is identical to the precursor, the process is transport with a maximum velocity of $k_{in} \; B_{max}$, symbolized by T_{max}. If the product is different from the precursor, the protein is an enzyme catalyst with the maximum reaction rate $k_{in} \; B_{max}$, symbolized by V_{max}.

Many processes retain transitional features, combining transport and catalysis, or binding and transport. The significance of the transitional processes depends on the relationship between the rate constants k_{off} and k_{in}. Little or no transport or catalysis takes places when k_{in} is equal or close to zero. Little or no binding occurs, on the other hand, when k_{off} is equal or close to zero. Thus, whether binding takes precedence over translocation or transformation depends on the relative rates of product release.

In principle, protein-ligand interaction does not fulfill the basic requirement of compartmental kinetics because the rate of relaxation depends on the concentration of the decaying substance. However, under special circumstances of the relaxation, depending on the magnitudes and time courses of the ligand concentrations, it is possible to define relaxation constants which reflect these circumstances. The following definitions are valid only when the ligand concentrations are effectively constant or nil, relative to their Michaelis constants, or when the total ligand occupancy of the receptors is constant. The distinction between the definitions does not apply to true steady-states, in which neither concentrations nor occupancies vary with time.

The common definitions of relaxation constants are based on the association constants,

$$k_1 = \left(1 - \sum \sigma\right) \frac{k_{\text{on}} B_{\max}}{V_1} \quad \text{and} \quad k_4 = \left(1 - \sum \sigma\right) \frac{k_{\text{out}} B_{\max}}{V_3} \tag{2.167}$$

are valid only when $\sum \sigma$ is constant or effectively nil and the concentration of any ligand varies as a function of time; in those cases, the dissociation constants are,

$$k_2 = k_{\text{off}} \quad \text{and} \quad k_3 = k_{\text{in}}. \tag{2.168}$$

while, *alternatively*, the less common definitions based on the dissociation constants,

$$k_2 = (1 + \chi_1)\, k_{\text{off}} \quad \text{and} \quad k_3 = (1 + \chi_3)\, k_{\text{in}} \tag{2.169}$$

are valid only when the concentrations of all ligands are constant and $\sum \sigma$ varies; in that case, the definitions based on the association constants are,

$$k_1 = \frac{k_{\text{on}} B_{\max}}{V_1} \quad \text{and} \quad k_4 = \frac{k_{\text{out}} B_{\max}}{V_3} \tag{2.170}$$

which cover the common test tube cases of build-up of bound substance from a constantly maintained medium but do not easily apply to living matter, in which changes of concentrations lead to changes of binding, rather than the reverse. It is important to keep in mind that the equations can be extended for any number of ligands in any combinations, some of which may be of constant concentration while others are effectively nil. At normal steady-state, all compartments have constant magnitudes. In that situation only the ratios between the relaxation constants have meaning, and neither set of definitions is valid.

Competitive Activation In competitive activation, the affinity of the binding sites for a ligand rises when another ligand binds to the same sites, i.e., the dissociation rates k_{off} and k_{in} decline. In the simplest way, the action is explained by the occupancy of the secondary ligand preventing the dissociation of the primary ligand for as long as the secondary ligand is bound. The occupancy of the ligand is then:

$$\sigma_1' = \frac{C_1}{K_{\text{M}_1}\,(1 - \sigma_3) + C_1} = \frac{C_1}{K_{\text{M}_1}' + C_1} = \frac{\chi_1\,(1 + \chi_3)}{1 + \chi_1\,(1 + \chi_3)} = \frac{\chi_1'}{1 + \chi_1'},$$

where $K_{\text{M}_1}' = K_{\text{M}_1}/(1 + \chi_3)$ and $\chi_1' = \chi_1\,(1 + \chi_3)$. The action of the secondary ligand changes the mass of bound ligand relative to the unbound ligand at steady-state expressed as the binding potential

$$p_{\text{B}_1}(\chi_1) = \frac{M_{2_1}}{M_1} = \frac{\sigma_1'\, B_{\max}}{M_1} = \frac{B_{\max}}{V_1\, K_{\text{M}_1}\,(1 + \chi_1 - \sigma_3)} = \frac{p_{\text{B}_1}(0)}{1 + \chi_1 - \sigma_3} \tag{2.171}$$

which predicts an increase of the binding potential in the presence of the secondary ligand. This equation also linearizes to the Eadie–Hofstee equation (Eadie 1952),

$$M_{2_1} = B_{\max} - [V_1 \; K_{\mathrm{M}_1} \; (1 - \sigma_3)] \; p_{\mathrm{B}_1}(\chi_1) \tag{2.172}$$

according to which the competitive activation reduces the magnitude of the Michaelis constant in proportion to the magnitude of activator concentration, χ_3, provided they are constant.

Non-Competitive Interaction

In noncompetitive interaction, the occupation of the sites by the noncompetitively interacting ligand is not influenced by the changing concentrations of other ligands, either because their concentrations are too low relative to their Michaelis constants ("tracers") or because the noncompetitively interacting ligand permanently renders particular sites unavailable to occupation by other ligands, i.e., lowers the association rate for other ligands so much that their concentrations are now insignificant relative to their noncompetitively elevated Michaelis constants. There are two kinds of noncompetitive interaction, inhibition and activation.

Non-Competitive Inhibition In noncompetitive inhibition, a fraction of the protein sites are permanently occupied by the inhibitor, regardless of the concentration of other ligands, or they are rendered permanently unavailable for occupation by any ligand. If the permanently unavailable sites are $\mathbf{M}_{2_3}$, the steady-state binding potential, obtained from (2.162) is,

$$p_{\mathrm{B}_1}(\chi_1) = \frac{M_{2_1}}{M_1} = \frac{\sigma_1 \; (1 - \varsigma_3) \; B_{\max}}{M_1} = \frac{(1 - \varsigma_3) \; B_{\max}}{V_1 \; K_{\mathrm{M}_1} \; (1 + \chi_1)} = \frac{1 - \varsigma_3}{1 + \chi_1} \; p_{\mathrm{B}_1}(0), \tag{2.173}$$

where ς_3 is now the occupancy of the noncompetitively interacting ligand, which is independent of the concentrations of other ligands. This equation also linearizes to the Eadie–Hofstee equation,

$$M_{2_1} = (1 - \varsigma_3) \; B_{\max} - V_1 \; K_{\mathrm{M}_1} \; p_{\mathrm{B}_1}(\chi_1) \tag{2.174}$$

which confirms that noncompetitive inhibition reduces the number of available binding sites, but leaves the affinity of the available sites intact.

As earlier, the corresponding definitions of relaxation constants for mixed competitive and noncompetitive interaction, i.e.,

$$k_1 = (1 - \sigma_1) \, \frac{k_{\mathrm{on}} \; (1 - \varsigma_3) \; B_{\max}}{V_1} \qquad \text{and} \qquad k_4 \cong 0 \tag{2.175}$$

are valid only when σ_1 is constant or effectively nil and the concentration of any ligand varies as a function of time; in those cases, the dissociation constants are,

$$k_2 = k_{\mathrm{off}} \qquad \text{and} \qquad k_3 = k_{\mathrm{in}}. \tag{2.176}$$

Alternatively, the less common definitions based on the dissociation constants, i.e.,

$$k_2 = (1 + \chi_1)\ k_{\text{off}} \quad \text{and} \quad k_3 = (1 + \chi_1)\ k_{\text{in}}$$

are valid only when the concentrations of all ligands are constant and σ_1 varies; in that case, the definitions based on the association constants are,

$$k_1 = \frac{k_{\text{on}}\ (1 - \varsigma_3)\ B_{\max}}{V_1} \quad \text{and} \quad k_4 \cong 0$$

which, as earlier, can be extended for any number of ligands in any combinations, some of which may be of constant concentration, while others are effectively nil.

Non-Competitive Activation In noncompetitive activation, the interaction is coupled to the presence of an activator which gives the ligand access to the binding sites. For example, transport of some solutes against a concentration gradient is directly or indirectly coupled to the breakdown of ATP. In these cases, the binding potential is given by:

$$p_{\text{B}_1}(\chi_1) = \frac{\sigma_1\ \varsigma_3\ B_{\max}}{M_1} = \frac{\varsigma_3\ B_{\max}}{V_1\ K_{\text{M}_1}\ (1 + \chi_1)} = \frac{\varsigma_3\ p_{\text{B}_1}(0)}{1 + \chi_1}, \tag{2.177}$$

where ς_3 is now the occupancy of the agonist. The interaction of G-proteins with G-protein-linked receptors is of this kind, being activated by the primary receptor ligand, e.g., dopamine. Likewise, the Eadie–Hofstee plot becomes,

$$M_{2_1} = \varsigma_3 B_{\max} - [V_1\ K_{\text{M}_1}]\ p_{\text{B}_1}(\chi_1) \tag{2.178}$$

and the relaxation constant is

$$k_1 = \frac{(1 - \sigma_1)\ k_{\text{on}}\ \varsigma_3\ B_{\max}}{V_1}$$

.

2.2.5 Receptor Binding

The protein is said to function primarily as a receptor for a single ligand type when $k_{\text{off}} \gg k_{\text{in}}$, and $K_{\text{M}_1} \cong K_{d_1}$ (see (2.161)). Thus, when the translocation of the ligand ("internalization") is minimal, only association and dissociation occur. This is the situation originally conceived by Michaelis and Menten (1913) who assumed that the entity later termed the Michaelis constant would equal the dissociation constant $k_{\text{off}}/k_{\text{on}}$ of the protein–ligand complex, because of near-equilibrium between $\mathbf{M_1}$ and $\mathbf{M_2}$. Subsequently, it was shown that this kind of near-equilibrium exists mostly in the cases of receptor binding. The interaction between a single ligand and the receptor protein is a simple exchange between two compartments (adapted from Fig. 2.2) as shown in Fig. 2.15:

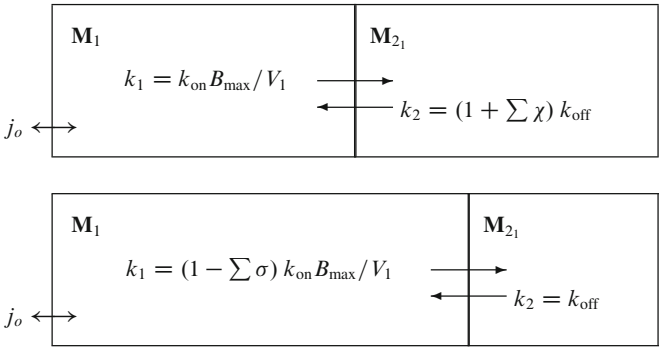

Fig. 2.15 Partial steady-states of free and bound ligand compartments established by receptor protein occupied by ligand m_1. Depending on individual steady-states, either *top* or *bottom* panel defines relaxation constants. Note that receptor protein may be occupied by other ligands also. *Top panel* requires constant ligand concentrations, *bottom panel* constant receptor occupancy

The main applications of the protein–ligand association equations for receptor binding are the determination of the maximum number of receptor sites, the affinity of the sites for the ligand, or the ligand's occupancy of the receptors. These determinations all involve the binding potential. The binding potential is obtained from the steady-state receptor binding given by the product of the steady-state ligand concentration and volume of distribution (2.21),

$$M_{2_1} = V_1 \left(\frac{k_1}{k_2}\right) C_1 = \frac{k_{on} B_{max}\ C_1}{k_{off}(1 + \sum \chi)} = \frac{B_{max}\ C_1}{K_{d_1}(1 + \sum \chi)} = \frac{B_{max}\ \chi_1}{1 + \sum \chi} = \sigma_1\ B_{max} \tag{2.179}$$

which is the formulation of the Michaelis–Menten equation for the binding of a ligand to its receptor. The ratio k_1/k_2 is the ligand's binding potential, according to (2.165),

$$p_{B_1}(\chi_1) = \frac{k_1}{k_2} \tag{2.180}$$

and its steady-state volume of distribution is $V_1\ (1 + [k_1/k_2])$. The maximum number of available sites, B_{max}, is related to the binding potential by rearrangement of (2.166),

$$M_{2_1} = B_{max} - [V_1\ K_{d_1}\ (1 + \chi_3)]\ p_{B_1}(\chi_1) \tag{2.181}$$

which is the Eadie–Hofstee equation of a line with slope $-V_1\ K_{d_1}\ (1 + \chi_3)$ and ordinate intercept B_{max} but only when the concentrations of all ligands other than m_1 are constant or effectively nil. The slope reflects the dissociation constant of the binding, the volume of distribution of the unbound ligand, and the concentrations (constant or nil) of all other ligands interacting with the receptors. The presence of other ligands affect the affinity and, therefore, the binding potential of the ligand in question.

2.2.6 Facilitated Diffusion

A protein can facilitate the diffusion of the ligand across a membrane when k_{in} is not negligible relative to k_{off}. The ligand usually remains intact during the translocation, but in principle may also undergo a chemical change. This process is important when the unassisted diffusion is slow, i.e., when the protein spans a membrane in which the diffusion coefficient of the ligand is low. Association and release obey the same equation as receptor binding but the predominant decay of the compartment occurs by release of the intact ligand from the compartment other than the one whence it originated. The translocation is unidirectional if the binding sites are accessible from only one compartment ("side"), here symbolized by $\mathbf{M}_1$. Spontaneous conformational change of the transporter protein makes the transporter accessible from alternating sides but the basic model has two compartments with a sink (Fig. 2.16, adapted from Fig. 2.3).

The flux and, hence, the relaxation constant depend on the concentration of the ligand. The maximum transport rate T_{max} is defined as $k_{in} B_{max}$. Hence the rate constants are,

$$k_1 = \left(1 - \sum \sigma\right) \frac{k_{on} B_{max}}{V_1} = \left(1 - \sum \sigma\right) \frac{k_{on} T_{max}}{k_{in}\, V_1} = \frac{(1 - \sum \sigma)\, T_{max}}{V_1\, (K_{M_1} - K_{d_1})}, \tag{2.182}$$

where the magnitude of $\sum \sigma$ depends on the simultaneous accessibility of the transporter from both sides of the membrane. The steady-state relaxation constant is a function of the partition coefficient as expressed in (2.33),

$$k_1' = k_{in}\; p_{B_1}(\chi_1) = \frac{(1 - \sum \sigma)\, k_{in}\; B_{max}}{V_1 K_{M_1}} = \frac{(1 - \sum \sigma)\, T_{max}}{V_1\; K_{M_1}} \tag{2.183}$$

provided $\sum \sigma$ reflects uniformly distributed ligands in true compartments. Because the presence of the transporter establishes an effective permeability for the ligand,

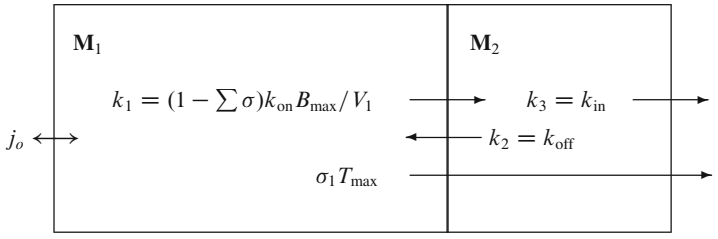

Fig. 2.16 Steady-state model of metabolite interaction with facilitating transport protein ($\mathbf{M}_2$). When p_{B_1} is binding potential, steady-state k_1' equals $k_{in}\, p_{B_1}$ and reaches $k_1 = k_{on} B_{max} / V_1$ when $k_{in} \gg k_{off}$

the steady-state relaxation constant of compartment $\mathbf{M}_1$ defines an apparent permeability in the direction of the net transport, P_1',

$$P_1' S = V_1\, k_1' = V_1\, k_{\text{in}}\, p_{\text{B}_1} = \left(1 - \sum \sigma\right) \frac{T_{\max}}{K_{\text{M}_1}}, \tag{2.184}$$

where the binding potential is now given by:

$$p_{\text{B}_1} = \frac{k_1}{k_2 + k_3} \tag{2.185}$$

such that the apparent permeability-surface area product now is,

$$P_1' S = V_1 \left(\frac{k_1 k_3}{k_2 + k_3}\right) \tag{2.186}$$

and the steady-state flux is a simple function of the ligand's occupancy,

$$J_1' = P_1' S C_1 = \left(1 - \sum \sigma\right) \left[\frac{T_{\max}}{K_{\text{M}_1}}\right] C_1 = \sigma_1\, T_{\max}, \tag{2.187}$$

where the evaluation of the influence of the ligand's concentration, i.e., the magnitude of the occupancy, uses the linear rearrangement of the Eadie–Hofstee (2.166),

$$J_1' = T_{\max} - \left[V_1\, K_{\text{M}_1} \left(1 + \sum \chi - \chi_1\right)\right] k_1' = T_{\max} - \left[K_{\text{M}_1} \left(1 + \sum \chi - \chi_1\right)\right] P_1' S, \tag{2.188}$$

where $T_{\max}$ is the ordinate intercept and $-V_1\, K_{\text{M}_1}\, (1 + \sum \chi - \chi_1)$ is the slope, provided the interactions are competitive.

Net Transport of Single Ligand

The net flux depends on the simultaneous accessibility of the transporter from both sides of the membrane. In the conventional *unidirectional* case, the transporter sites are accessible only from one side of the membrane at a time and hence enjoy a higher occupancy of the ligand on that side, while in the *bidirectional* case, the transporter sites are accessible from both sides at the same time and hence have lower degrees of saturation from either side.

In the case of the unidirectional transporter, the transporter sites can be accessed by several ligands but only from the same side of the membrane at any one time. If only a single ligand is present in the precursor compartment, as in the case of glucose and the GLUT1 transporter (Gjedde 1992), (2.184) is modified to,

$$P_1' S = \frac{(1 - \sigma_1)\, T_{\max}}{K_{\text{M}_1}} = \frac{T_{\max}}{K_{\text{M}_1} + C_1} \tag{2.189}$$

and the flux of the uniformly distributed substrate, facilitated by the unidirectional action of the transporter, equals,

$$J_1' = V_1\, k_1'\, C_1 = P_1' S\, C_1 = \sigma_1\, T_{\max} \tag{2.190}$$

and in the opposite direction, provided $k_{\text{off}} = k_{\text{in}}$, i.e., when $T_{\max}$ is the same in the two directions,

$$J_3' = V_3\, k_4'\, C_3 = P_3' S\, C_3 = \frac{T_{\max}\, C_3}{K_{M_3} + C_3} = \sigma_3\, T_{\max} \tag{2.191}$$

which implies a different apparent permeability, dictated by the magnitude of C_3 relative to C_1, and the difference in turn affects the magnitude of the distribution volume. The net transport is the difference between the fluxes in the two directions,

$$J_1' = (\sigma_1 - \sigma_3)\, T_{\max} = f_b{}'\, \sigma_1\, T_{\max}, \tag{2.192}$$

where $1 - f_b{}'$ is now the ratio between the different occupancies of the ligand on the two sides of the interface, established by the saturable nature of the binding to the transporter, rather than simply being the ratio between the concentrations as in (2.119).

Facilitated diffusion is in principle passive, i.e., non-energy requiring. In case of active, energy-requiring transport against a concentration gradient, the ligand can be translocated by association with sites activated by another ligand which itself may or may not be translocated. The occupancy of the ligand in question may be low, yet net transport proceeds against a concentration gradient because more sites are made available for the ligand at the low concentration than for the ligand at the high concentration on the opposite side of the interface. The activation is reflected in the definition of $f_b{}'$, when $\sigma_1\, \varsigma_1 > \sigma_3\, \varsigma_3$,

$$f_b{}' = 1 - \frac{\sigma_3\, \varsigma_3}{\sigma_1\, \varsigma_1}$$

in which the low occupancy of M_1 (σ_1) is compensated by the high occupancy (ς_1) of the activating ligand (Fig. 2.17).

Flow-Limited Net Transport of Single Ligand

Equation (2.189) raises the issue of the distribution of the ligand in the delivery compartment, when this compartment is the vascular bed. Not only are the apparent permeabilities different for the two directions of transport but they also vary along the length of the capillary because of the decline of the ligand concentration, as the ligand is delivered to the exchange compartment. Gjedde (1980) treated the case of the varying apparent permeability of the blood–brain barrier to glucose and showed

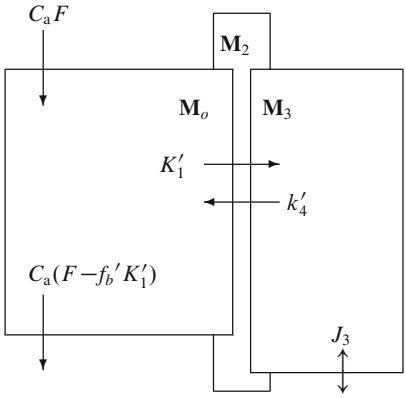

Fig. 2.17 Compartmental model of capillary and tissue compartments in which tissue compartment clears solute such as glucose from plasma flowing through capillary compartment by means of unidirectional GLUT1 transporters. The fraction $1 - f_b'$ is the ratio between effective concentrations of glucose in tissue and capillary compartments, caused by higher apparent permeability in direction from tissue to capillary because of lower glucose concentration. Primes refer to net transport through membranes of $\mathbf{M}_2$

that the effect can be ignored when the extraction is low (Gjedde 1980). The analysis showed that the decrease of the ligand concentration, as blood passes along the capillaries, has little influence on the magnitude of the apparent permeability when the ratio $J_1'/[F(K_{M_1} + C_1)]$ is less than 0.1, where F is blood flow, i.e., when $f_b'\sigma_1 P_1' S/F < 0.1$. Thus, it is approximately correct to modify (2.192) for the apparent permeability generated by the facilitated diffusion, as illustrated earlier,

$$J_1' \cong f_b' C_a \, F \left(1 - e^{-P_1' S/F}\right) = f_b' \, K_1' \, C_a \,, \tag{2.193}$$

where C_a is the arterial glucose concentration, and K_1' is the apparent clearance established by the presence of the permeability symbolized by $P_1' S$, the prime referring to the net transport through the two membranes of the endothelium.

The error incurred by ignoring the effect of the changing substrate concentration is revealed by the formula for the average capillary concentration of the ligand (2.151),

$$\overline{C}_1 = C_a \left[1 - f_b' \left(1 - \frac{1 - e^{-P_1' S/F}}{P_1' S/F}\right)\right], \tag{2.194}$$

where the relationship between $\overline{C}_1$ and C_a depends on the magnitudes of f_b' and the $P_1' S/F$ ratio. The ratio of the occupancies of the ligand on the two sides of the interface can be inferred from the ratio between the "unidirectional" and net fluxes at steady-state,

$$f_b' = \frac{J_3}{C_a \, K_1'} = \frac{K'}{K_1'}, \tag{2.195}$$

where K' is the net clearance. This ratio is approximately 0.5 for the transport of D-glucose across the human blood–brain barrier, indicating that the occupancy on the tissue side of the interface is half of that in plasma and the concentration in the tissue water one-third of that in plasma (Gjedde 1995a).

Flow-Limited Net Transport of Multiple Ligands

Equation (2.193) is valid also when multiple ligands are present in the precursor compartment, as in the case of the transporter of large neutral amino acids (LeFauconnier 1992). Changes of the apparent permeabilities on the two sides are then buffered by the large number of ligands. The net flux is given by the equation,

$$J_1 \cong K_1' \, C_\mathrm{a} \left(1 - \frac{\sigma_3}{\sigma_1}\right) = f_b' \, K_1' \, C_\mathrm{a}, \tag{2.196}$$

where, to recapitulate, $1 - f_b'$ is the ratio between the occupancies on the two sides of the interface (the prime referring to facilitated rather than simple diffusion), K_1' the rate of clearance from the virtual compartment $\mathbf{M}_o$ through compartment $\mathbf{M_2}$ to compartment $\mathbf{M_3}$ in the direction from vessel to tissue, and C_a is the arterial concentration of the ligand, equal to the uniform concentration of the ligand in $\mathbf{M_0}$. The net translocation ceases when the occupancies are the same on the two sides. Multiple ligands, on the other hand, may influence the translocation indirectly by changing the occupancy of the ligand on one or both sides.

2.2.7 Enzymatic Reactions

The protein is said to be an enzyme when the product is different from the precursor and physical translocation of the product is not a main function of the protein. The action of the protein may or may not involve translocation, and the sites usually are accessible by both product and precursor, although not at the same time. The model is adapted from Fig. 2.5 (Fig. 2.18).

The maximum rate of the enzymatic reaction (V_max) is $k_\mathrm{in} B_\mathrm{max}$. Thus,

$$k_1 = \left(1 - \sum \sigma\right) \frac{k_\mathrm{on} B_\mathrm{max}}{V_1} = \left(1 - \sum \sigma\right) \frac{k_\mathrm{on} V_{\mathrm{max}_1}}{k_\mathrm{in} \, V_1} = \frac{(1 - \sum \sigma) \, V_{\mathrm{max}_1}}{V_1 \, (K_{\mathrm{M}_1} - K_{d_1})}, \tag{2.197}$$

where the magnitude of $\sum \sigma$ depends on the number of substrates and inhibitors accessed by the enzyme. The steady-state relaxation constant in the direction from

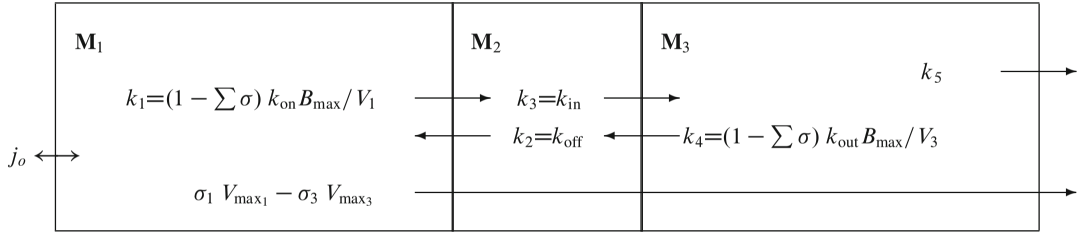

Fig. 2.18 Model of precursor and product compartments separated by enzyme ($\mathbf{M}_2$) occupied by precursor (m_1) and product (m_3). Reaction sites are not accessed by precursor and product at same time

precursor to product is a function of the affinity of the enzyme for the precursor as expressed in (2.167),

$$k_1' = \frac{(1 - \sum \sigma)\ k_{\text{in}}\ B_{\max}}{V_1\ K_{\text{M}_1}} = \frac{(1 - \sum \sigma)\ V_{\max_1}}{V_1\ K_{\text{M}_1}} \tag{2.198}$$

provided the precursor is uniformly distributed in the compartment. Likewise, the steady-state relaxation constant in the direction from product to precursor is a function of the affinity of the enzyme for the product,

$$k_4' = \frac{k_{\text{off}}\ B_{\max}}{V_3\ K_{\text{M}_3}} = \frac{(1 - \sum \sigma)\ V_{\max_3}}{V_3\ K_{\text{M}_3}} \tag{2.199}$$

provided the product is also uniformly distributed in the compartment. The relaxation constant for an enzymatic reaction is often referred to as the enzyme activity, i.e., the maximum rate relative to the K_{M} and corrected for volume of distribution (V_1) and presence of competitors ($\sum \sigma$). The actual rate of the enzymatic reaction is then,

$$J_1' = \sigma_1\ V_{\max_1} - \sigma_3\ V_{\max_3} = f_b'\ \sigma_1\ V_{\max_1}, \tag{2.200}$$

where $1 - f_b'$ is now the ratio $\sigma_3 V_{\max_3}/[\sigma_1 V_{\max_1}]$, that is, not only a function of the affinity of the enzyme and concentration of the ligand but also of the maximum rate in both directions of the transformation. This is the general form of the Michaelis–Menten equation.[2]

If the net flux is close to zero, this relationship may be difficult to establish. The reaction then is said to be near-equilibrium. In this case, the ratio of the precursor and the substrate is a simple function of the ratio between the dissociation constants at steady-state,

$$\frac{C_3}{C_1} = \frac{K_{\text{M}_3} V_{\max_1}}{K_{\text{M}_1} V_{\max_3}} = \frac{k_{\text{in}}\ k_{\text{on}}}{k_{\text{out}}\ k_{\text{off}}} = \frac{K_{d_3}}{K_{d_1}} \tag{2.201}$$

which may differ for different precursors and substrates, as both K_{M} and $V_{\max}$ magnitudes vary among precursors and substrates. At near-equilibrium, fluxes in the two directions are of similar magnitude as well as much greater than the net reaction rate. This contrasts with nonequilibrium steady-state, where concentrations are constant and fluxes in the two directions are very different.

---

[2] Although f_b' varies with the occupancies of precursor and product, magnitudes of $V_{\max_1}$ and an apparent K_{M_1} can be related by the Eadie–Hofstee equation (Eadie 1952; Hofstee 1952),

$$J_1' = V_{\max_1} - \left[V_1\ K_{\text{M}_1}\left(1 + \left[\frac{C_3}{K_{d_3}}\right]\right)\right] k_1',$$

where $V_{\max_1}$ is the ordinate intercept and $-V_1\ K_{\text{M}_1}(1 + [C_3/K_{d_3}])$ is the slope, provided C_3 is constant. The relationship implies that the bidirectional exchange influences the apparent Michaelis constant.

2.3 Determination of Relaxation Constants

2.3.1 Stimulus-Response Relations

The purpose of the kinetic analysis is to deconvolve the characteristic constants of the impulse response function from the relationship between a perturbation of the steady-state of a system of compartments and the time-course of its return to steady-state. The perturbation of the steady-state usually consists in an induced change of the contents of the delivery compartment ("stimulus"). The subsequent return to steady-state ("response") is recorded as timed measurements of the contents of the entire system under investigation. Under certain limited circumstances, the use of tracers allows investigators to estimate the magnitude of relaxation constants and derived variables (clearance and volume of distribution) by deconvolving the impulse response function from one or more solutions of the differential equations which predict the response of the compartments to the stimulus.

Generally, tracers are labeled molecules that enter compartments without affecting the magnitude of the relaxation constants which define the compartments. Tracers are designed to have the same physical properties as the native molecules but to exist in such low concentration that the total number of molecules in the compartment is constant. This characteristic is not always fulfilled, however, because the tracer molecules may differ from the native molecules in their chemical properties, particularly with respect to the magnitude of affinities, and dissociation and Michaelis constants. For this reason, it is often necessary to carefully distinguish between relaxation constants, which follow the exchanges of the native molecules, and relaxation constants which describe the exchanges of the tracers.

When tracer molecules enter a compartment, the underlying assumption is that they are chemically indistinguishable from the native members of the compartment from the point of view of the mechanism responsible for the relaxation. Here, the tracer molecules in any compartment are symbolized by m^* and their concentration in the compartment by c^*.

By definition, tracers rarely reach steady-state. Eventually, they disappear by decay or washout, unless they are continuously supplied, or neither decay nor escape from the compartments where they end up. The transient solutions are therefore useful to the estimation of relaxation constants, provided the predicted solutions of the differential equations are sufficiently accurate. The significance of this accuracy is the object of the regression analysis.

The methods fall into three categories, the single-bolus nonlinear deconvolutions, the steady-state programmed infusions, and the multiple-time graphical analyses. The deconvolutions are accurate but potentially imprecise and offer no directly verifiable results. The infusions are designed to let the tracer reach steady-state in extended periods of time. The multiple-time graphical analyses combine the advantage of the bolus injection with the visibility of the infusion results.

2.3.2 Regression Analysis

Regression vs. Function Analysis

The purpose of regression analysis is to establish the relations between two sets of variables, in the current context between the timed measurements of tracer concentration or content in a delivery compartment, say $\mathbf{M}_1$, and the timed measurements of tracer concentration in a number of tissue compartments, $\mathbf{M}_2$ to $\mathbf{M}_n$, often including the delivery compartment. The relationship between the two sets of variables is established in the form of a model with a number of constants, parameters, the magnitudes of which are unknown (model-based regression), or in the form of a class of equations (basis-functions) with known coefficients applicable to a system of compartments, the number and structure of which must be deduced from the data (data-based function analysis). The regression relation is based on the variations of both the "true" values of the variables and the random errors to which the observations of these variables are subject. The functional relations, on the other hand, depend on the variation of "true" values of these variables only, stripped of the random errors associated with their observation.

Regression Analysis The conventional regression analysis assumes a model solution and delivers estimates of the magnitude of the parameters that are most consistent with the known model. The regression analysis indicates with a certain statistical probability the range of values of the parameters which are consistent with the chosen model. As the relationship in principle is either nonlinear or linear (i.e., uni- or multilinear), regression analyses are likewise either nonlinear or linear (i.e., uni- or multilinear). Non-linear regression analysis is still an imperfect art with many pitfalls, while linear regression analysis both conceptually and mathematically is simpler. While nonlinear regression analysis proceeds by iteration until a given threshold of accuracy is reached, linear regression analysis often can be completed in a single analytical step. The disadvantage of linear regression, on the other hand, is that it can be subject to important bias, which must be taken into account.

The importance of the parameter estimates must be established by statistical tests, which are frequently misinterpreted. The problem is that a parameter estimate may have been established within satisfactorily narrow limits, yet may express no more than the noise inherent in the measured variables. Another parameter estimate may have been established within fairly wide limits, yet may represent a very accurate estimate of the biological variability of the measured variables. For these and other reasons, it is important to distinguish between precision and accuracy, also in terms of their practical applicability. Accuracy may be useless if the variables indeed are subject to unavoidable biological variation, while precision may be useful as an indicator of the difference among several sets of data, despite the bias of the estimates.

Basis Function Analysis The data-driven basis-function analysis assumes a set of parameters of known magnitude and chooses the model configuration most consistent with the data. This approach is a search for the optimal structural relations among compartments which predict the form of the response function. As an intriguing consequence it is possible to fit combinations of models to the data. These model solutions are "probabilistic" in the sense that the resulting model structure can be established only with a finite probability of consistency with the data. The analysis is not an actual deconvolution but rather a segmentation of the data in probablistic clusters of model structure.

Model-Based Deconvolution

In seeking the regression relation between two sets of tracer measurements, $c^*(t)$ and $m^*(t)$, the values of the dependent variable m^* are presumed to be randomly distributed about the regression function, so that its *expected* values are known to be a specific function of the *observed* values of the independent variable c^*. The expected values of the dependent variable m^* are the function $\overline{m}(c^*(t), t, p_1, ..., p_n)$, where $p_1, ..., p_n$ refers to the n parameters of the functional relation. If the distribution of $m^*(T)$ (where T is a time of observation) about $\overline{m}(c^*(T), T, p_1, ..., p_n)$ is normal for all T, the method of Least Squares is the most efficient means of estimating the parameters. The sum of squares to be minimized is,

$$S_{\text{sq}} = \sum_{i=a}^{b} \left[m^*(T_i) - \overline{m}(c^*(T_i), T_i, K_1, k_2, ..., k_n) \right]^2 , \tag{2.202}$$

where a and b define a range of measurements chosen to ensure sufficient degrees of freedom in relation to the number of parameters. The minimization is carried out by means of differential calculus but it can be performed by elementary algebra in the cases of linear and multilinear regression in a way which gives simultaneously the estimates of the parameters and the minimal sum of the squares. These methods will not be discussed here, as a large number of commercially available programs efficiently carry out the necessary computations.

In regression analyses of model parameters, it is common to refer to the "virtual" first compartment, $\mathbf{M}_o$, as the *delivery compartment* and the second compartment, $\mathbf{M}_2$, as the *precursor* or exchange compartment. The subsequent compartments, $\mathbf{M}_3$-$\mathbf{M}_n$, are then the *product compartments*. The concentration of the tracer precursor, $c_1^*(0)$, in the delivery compartment is c_{a}^*, which denotes the arterial concentration when the delivery compartment is the capillary bed. The tracer content of the precursor compartment is then m_{e}^* and the content of all the subsequent compartments is m_p^*. The sum of all compartments, $V_o c_{\text{a}}^* + m_{\text{e}}^* + m_p^*$, is then m^*. For three compartments, the tracer content obeys (2.43). The regression analysis then yields the parameter estimates, which minimize the sum of squares, and determines the residual sum of squares.

Data-Driven Basis-Function Analysis

In general, linear first-order differential equations define a system with an infinite number of compartments distinguished by the magnitude of their exponentials. An experimentally relevant subset of the compartment can be identified by means of least-squares fitting of the basis functions to the data (Gunn et al. 2001). The convolution of the impulse response function with the vascular or tissue forcing function leads to the actually observed tissue curve predicted by (2.16). The underlying impulse response function is assumed to be represented as a cluster of elements picked from a sufficiently large ("overcomplete") pool of pairs of preselected coefficients (K_{1_h}) and relaxation constants (k_{2_h}) assumed to include all of the actual compartments of the system. As standard least-squares analysis does not apply when the number of parameters exceeds the number of measurements, addition of a penalty function reduces the number of permitted elements to one which minimizes the penalty function. The penalty function depends on the variability of the data, expressed in the magnitude of the regularization term μ. The variability coefficient can be determined by any one of several methods of "denoising" or "smoothing" (Gunn et al. 2002). Greater variability of the data allows fewer elements in the cluster of compartments and prevents both overfitting and underfitting of the data (Shao 1993; Hjorth 1994),

$$S_{\mathrm{sq}} = \sum_{i,h=a,1}^{b,n-1} \Big(\big[m^*(T_i) - \overline{m}(c^*(T_i), T_i, K_{1_h}, k_{2_h}) \big]^2 + \mu_h \Big), \tag{2.203}$$

where μ is the regularization term.

2.3.3 *Deconvolution of Response Function by Differentiation*

In the cases of more than three or four compartments, the number of parameters is so great that regression analysis fails to identify a meaningful and unique set of estimates. In these cases it is possible to use the regression analysis to identify a precursor compartment because it regulates the influx to all of the subsequent compartments.

Using the substitution m^* for the total contents of the precursor and product compartment, c_{a}^* for $c_1(0)$, and V_o for the volume of the "virtual" capillary compartment defined in (2.150), the total flux of a labeled substance into any closed system of compartments is given by (2.73),

$$\frac{\mathrm{d}m^*}{\mathrm{d}t} = V_o \, \frac{\mathrm{d}c_{\mathrm{a}}^*}{\mathrm{d}t} + K_1 \, c_{\mathrm{a}}^* - k_2 \, m_{\mathrm{e}}^*, \tag{2.204}$$

where asterisks denote the labeled substance ("tracer"). When tracers are introduced into living tissue, the tracer precursor and its products distribute in separate compartments, which cannot be probed individually. The purpose of the regression is

to determine the individual time courses of the precursor and the products. Among other applications, this regression is used to determine true steady-state values of a binding potential (p_{B}), and the corresponding steady-state magnitude of bound tracer. The regression is based on the claim that the tracer flux into the tissue is driven by the concentration difference between the tracer contrations in the capillary circulation and the tissue with which the capillary is directly exchanging (precursor compartment). Equation (2.204) can be solved for the tracer content of the precursor (exchange) compartment,

$$m_e^* = V_{\mathrm{e}} \left[c_a^* - \frac{1}{K_1} \left(\frac{\mathrm{d}m^*}{\mathrm{d}t} - V_o \frac{\mathrm{d}c_a^*}{\mathrm{d}t} \right) \right], \tag{2.205}$$

where $V_{\mathrm{e}} = K_1/k_2$ is the partition volume. To obtain an estimate of the quantity of exchangeable tracer, it is necessary to determine the derivatives of m^* and c_a^*, and the magnitudes of V_o, V_{e}, and K_1.

To differentiate the function underlying the observed values m^*, the function must first be optimized by any suitably realistic formula, which minimizes the sum of squares but also has the property that the observed values maintain normal distribution about the optimized values of this formula. A degree of smoothing must be performed to allow differentiation with minimal variability. Equations (2.43) and (2.48) are recommended for this smoothing. With (2.43), the smoothing is accomplished by ordinary six-parameter nonlinear regression to the measured pairs of m^* vs. c_a^*. With (2.48), the best estimate of the expected ("smoothed") value $\overline{m}$ is calculated by an appropriate method of "denoising." One approach is to apply a differentiable function directly,

$$\overline{m} = a_1 c_{\mathrm{a}}^* + a_2 \int_o^T c_{\mathrm{a}}^* \,\mathrm{d}t + a_3 \int_o^T \int_o^u c_{\mathrm{a}}^* \,\mathrm{d}t \,\mathrm{d}u + a_4 \int_o^T m^* \,\mathrm{d}t + a_5 \int_o^T \int_o^u m^* \,\mathrm{d}t \,\mathrm{d}u, \tag{2.206}$$

where $\overline{m}$ is the optimized value, and the coefficients are those defined for (2.48).

Analytic Differentiation The nonlinear smoothing by means of (2.43) has the advantage that the derivatives of the function are analytically known in advance. Using the parameter estimates $\overline{k}_2$, $\overline{k}_3$, and $\overline{k}_4$, the expected quantity of tracer precursor is calculated from the relationship given in (2.39),

$$\overline{m}_{\mathrm{e}} = V_{\mathrm{e}} \, \overline{k}_2 \, \overline{\zeta}(t), \tag{2.207}$$

where V_{e} is the partition volume measured in a reference region and $\overline{\zeta}(t)$ is the expected function $\overline{m}_{\mathrm{e}}/K_1$ calculated from (2.39),

$$\overline{\zeta}(t) = \left(\frac{\overline{q}_2 - \overline{k}_4}{\overline{q}_2 - \overline{q}_1} \right) \int_o^T c_a^* \, \mathrm{e}^{-\overline{q}_2 \,(T-t)} \,\mathrm{d}t - \left(\frac{\overline{q}_1 - \overline{k}_4}{\overline{q}_2 - \overline{q}_1} \right) \int_o^T c_a^* \, \mathrm{e}^{-\overline{q}_1 \,(T-t)} \,\mathrm{d}t, \tag{2.208}$$

where $\overline{q}_1$ and $\overline{q}_2$ are calculated from the estimates $\overline{k}_2$, $\overline{k}_3$, and $\overline{k}_4$ by means of (2.40) and (2.41).

Numerical Differentiation Simple differentiation of (2.206) (Wong et al. 1998a) yields the flux into the precursor and product compartments required for determination of $\overline{m}_{\mathrm{e}}$,

$$\overline{j}_1 = \frac{\mathrm{d}m^*}{\mathrm{d}t} - a_1 \frac{\mathrm{d}c_{\mathrm{a}}^*}{\mathrm{d}t} = a_2\, c_a^* + a_3 \int_o^T c_{\mathrm{a}}^*\, \mathrm{d}t + a_4\, m^* + a_5 \int_o^T m^*\, \mathrm{d}t \quad (2.209)$$

such that (2.205) becomes,

$$\overline{m}_{\mathrm{e}} = V_{\mathrm{e}} \left[c_a^* - \frac{\overline{j}_1}{a_1 a_4 + a_2} \right], \quad (2.210)$$

where V_{e} is known from separate measurement of the tracer's partition volume (K_1/k_2) in a reference region, and where the relations following (2.48) have been used to derive the denominator, $a_1 a_4 + a_2$.

Determination of Precursor–Product Ratio (Binding Potential) The tracer product is the precursor subtracted from the total,

$$\overline{m}_p = \overline{m} - \overline{m}_{\mathrm{e}} - a_1\, c_{\mathrm{a}}^*,$$

where $\overline{m}$ is the time-activity curve in the region of interest, smoothed according to (2.206)(Wong et al. 1998a). At the peak of $\overline{m}_p$, $\mathrm{d}\overline{m}_p/\mathrm{d}t$ is zero and $\overline{M}_p$ is at steady-state (transient equilibrium). The precursor–product ratio (steady-state binding potential), p_{B}, is the ratio between $\overline{M}_p$ and $\overline{M}_e$ at this time only (indicated by upper-case symbols),

$$p_{\mathrm{B}} = \frac{\overline{M}_p}{\overline{M}_e} = \frac{\overline{M} - V_o C_{\mathrm{a}}^*}{\overline{M}_e} - 1, \quad (2.211)$$

where V_o is the estimate of a_1 in the case of the multilinear regression by (2.206) as shown in Wong et al. (1998a). The quantity of tracer product at the peak is determined as the ratio between $\overline{M}_p$ and the specific activity A (Fig. 2.19),

$$M_p = \frac{\overline{M}_p}{A}.$$

2.3.4 Deconvolution by Temporal Transformation

Constant Forcing Function

The deconvolution of the response function by means of temporal transformation is based on the properties of (2.74) when c_{a}^* is maintained constant (i.e., symbolized by C_{a}^*),

$$v^*(T) \equiv \sum_{i=1}^{n} \frac{m_i^*(T)}{C_{\mathrm{a}}^*} = V_o + \sum_{h=1}^{n-1} \left[\frac{K_{1_h}}{k_{2_h}} \left(1 - \mathrm{e}^{-k_{2_h} T} \right) \right],$$

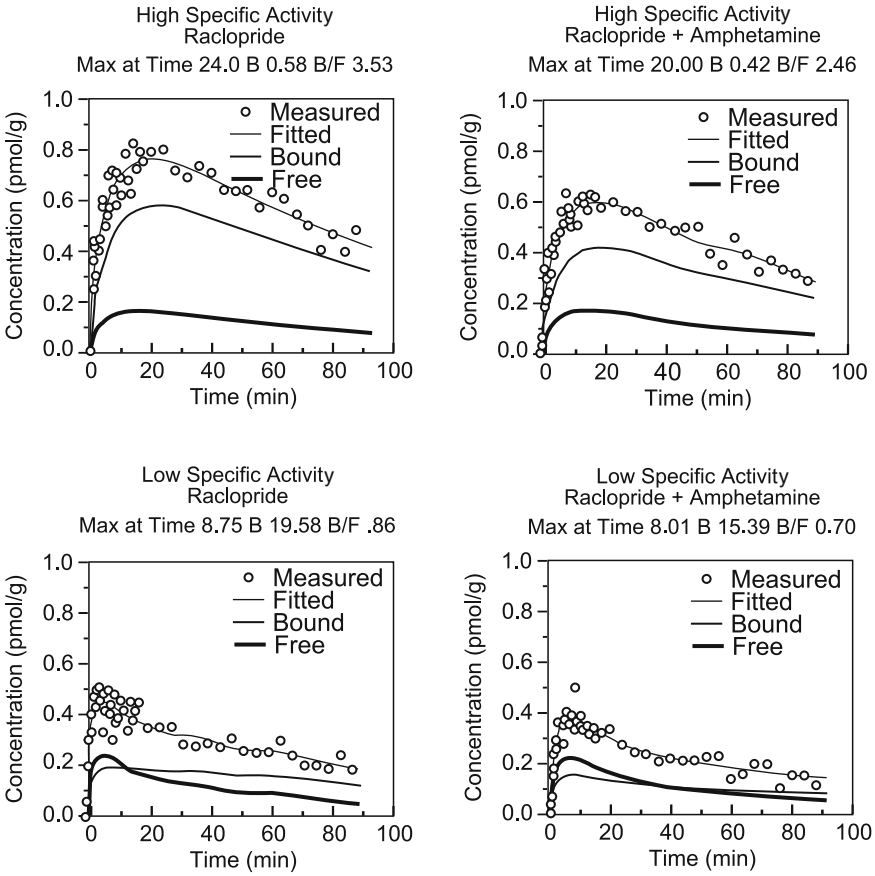

Fig. 2.19 Precursor and product curves at high (*top panels*) and low (*bottom panels*) specific activies before (*left panels*) and after (*right panels*) competitor (dopamine released amphetamine) action. Resulting estimates for the upper left-hand panel are listed in Table 2.2. From Wong et al. (1998a)

where $v^*(T)$ is the apparent volume of distribution as a function of time (T). The equation simplifies to the equation,

$$v^*(T) = V - \sum_{h=1}^{n-1} \left[\frac{e^{-k_{2_h} T}}{k_{2_h}} \right],$$

where V is the total steady-state volume of distribution. The behavior of the equation depends on the relationship between k_{2_h} and T. For values of $T \ll 1/k_{2_h}$ for all h,

$$v^*(T) = V_o + T \sum_{h=1}^{n-1} K_{1_h} = V_o + K_1 T$$

which has the properties of a straight line and is a special case of (2.21) for constant c_1. For values of $T \gg 1/k_{2_h}$ for all h,

$$v^*(T) = V_o + \sum_{h=1}^{n-1} \frac{K_{1_h}}{k_{2_h}} = V = V_o + \sum_{h=1}^{n-1} V_h$$

which is a steady-state plateau equivalent to the level defined by (2.22). For intermediate values of T, $1/k_{2_h} \ll T$ for $h < g$ and $1/k_{2_h} \gg T$ for $h \geq g$, the intermediate equation results,

$$v^*(T) = V_o + \sum_{h=1}^{g-1} V_h + T \sum_{h=g}^{n-1} K_{1_h} = V_o + \sum_{h=1}^{g-1} V_h + K\,T \tag{2.212}$$

which is a straight line with an ordinate intercept and a slope of K, formally equivalent to (2.84). The equivalence indicates that normalization of the integrated forcing function compensates for nonlinearity of the forcing function. The normalization has unit of time and represents a temporal transformation.

The use of the transformed time as independent variable, and the volume v^* as the dependent variable, changes the time course of the response and allows inference ("graphical analysis") to be made of the steady-state clearance of the tracer.

Variable Forcing Function

In analogy with (2.21) and (2.84), the primary temporal transformation creates a new time variable in the case of a variable forcing function,

$$\Theta^*(T) = \frac{\int_o^T c_\mathrm{a}^*\,\mathrm{d}t}{c_\mathrm{a}^*(T)}$$

as does the secondary temporal transformation,

$$\Theta'^*(T) = \frac{\int_o^T \int_o^u c_\mathrm{a}^*\,\mathrm{d}t\,d\,u}{\int_o^T c_\mathrm{a}^*\,\mathrm{d}t}. \tag{2.213}$$

Also judging from the equivalence with (2.21) and (2.84), the primary dependent variable is an apparent partition volume,

$$v^*(T) = V_o + \sum_{i=2}^{n} v_i^* = \sum_{i=1}^{n} \frac{m_i^*}{c_\mathrm{a}^*}$$

and the secondary dependent variable an apparent partition volume which approaches the steady-state volume of distribution, i.e., the integral of the impulse response function, when time approaches infinity,

$$v'^*(T) = V_o + \sum_{i=2}^{n} v_i^* = V_o + \sum_{i=2}^{n} \frac{\int_o^T m_i^* \, \mathrm{d}t}{\int_o^T c_\mathrm{a}^* \, \mathrm{d}t} \tag{2.214}$$

which has the special significance of being the ratio of the total areas under the curves of the response and the stimulus. The fact that this ratio approaches the steady-state volume of distribution as T approaches infinity, is the *stimulus-response theorem* (Lassen and Perl 1979).

Graphical Analysis of Primary Temporal Transformation

For n compartments, the expected results of the multilinear solution to (2.204) are given by (2.74):

$$m^*(c_\mathrm{a}^*, m_\mathrm{e}^*) = V_o \, c_\mathrm{a}^* + K_1 \int_o^T c_\mathrm{a}^* \, \mathrm{d}t - k_2 \int_o^T m_\mathrm{e}^* \, \mathrm{d}t,$$

where m_e^* is the tracer content of the precursor compartment. The earlier equation rearranges to,

$$\frac{m^*}{c_\mathrm{a}^*} = V_o + K_1 \int_o^T \left[\frac{c_\mathrm{a}^*(t)}{c_\mathrm{a}^*(T)}\right] \mathrm{d}t \left(1 - \left[\frac{k_2 \int_o^T m_\mathrm{e}^* \, \mathrm{d}t}{K_1 \int_o^T c_\mathrm{a}^* \, \mathrm{d}t}\right]\right)$$

and, thus, to the temporally transformed equation,

$$v^*(T) = V_o + K_1 \, \Theta^* \left(1 - \left[\frac{v_e'^*(T)}{V_\mathrm{e}}\right]\right), \tag{2.215}$$

where $v_e'^*(T)$ is the apparent partition volume at time T.

Two Compartments For two compartments, (2.215) reduces to the Gjedde–Patlak plot (2.21) for all times T for which $v_e'^*(T) \ll V_\mathrm{e}$,

$$v^*(T) = V_o + K_1 \, \Theta^*. \tag{2.216}$$

Multiple Compartments With continued incremental accumulation of at least one product (m_p^*), Gjedde (1982) showed that (2.216) reduces to (2.84) also for multiple compartments, provided steady-state exists between the delivery and precursor compartments. Thus, when it is true that the ratio $V_\mathrm{e}'^*(T)/V_\mathrm{e}$ maintains a constant ratio less than unity but greater than zero, it is also true that

$$m_p^*(T_2) - m_p^*(T_1) = K \, \big(\Theta^*(T_2) - \Theta^*(T_1)\big), \tag{2.217}$$

where K is the net clearance of the precursor to at least one of several product compartments, relative to the concentration of the precursor in the circulation. The general Rutland–Gjedde–Patlak Equation (2.218) is then valid,

$$v^*(T) = V_o + \sum_{i=2}^{n} V_i + K\ \Theta^* = V_n + K\ \Theta^*, \tag{2.218}$$

where V_n is a "virtual" precursor volume of distribution. The precursor volume is "virtual" because it does not actually contain the precursor from the onset of the uptake but from the onset of the steady-state (secular equilibrium) between the delivery and precursor compartments.

The lumped variables (2.213) define linear relationships applicable to results from in vivo or ex vivo tomography, including autoradiography, positron emission tomography, and magnetic resonance spectroscopy.

Graphical Analysis of Secondary Temporal Transformation

The apparent partition volume $v'^*(T)$ is the ratio of the areas under the response function and the forcing (stimulus) function curves (AUC). The analysis extends the graphical analysis, which can be useful also in the absence of measurements of a proper vascular forcing function. The method extends the graphical analysis by integrating delivery and precursor–product curves prior to the normalization. As with the simple ratios, the independent variable has unit of time, and the new dependent variable is the ratio between the integrals of the total content of the precursor and product compartments and the integral of the tracer concentration of the delivery compartment.

Vascular Forcing Function The approach to the ratio of integrated compartments employs the temporally transformed independent variable Θ', equal to $\int_o^T \int_o^u c_a^* \mathrm{d}t\, du / \int_o^T c_a^* \mathrm{d}t$. The AUC analysis is applicable to models with any number of compartments, but the interpretation of the ratios of the areas under the curves depends on the model.

The model shown in Fig. 2.20 is an example of a model which can be analyzed by the AUC analysis. $\mathbf{M}_o$ is the virtual delivery compartment, in which the tracer concentration is c_a^*. It masks the real delivery compartment, which does not fulfill the fundamental compartment criteria as discussed earlier. $\mathbf{M}_2$ is the precursor compartment and $\mathbf{M}_{3_1}$ and $\mathbf{M}_{3_2}$ are the irreversible and reversible accumulation compartments, respectively. It is further assumed that the relaxation constants k_{3_2} and k_{4_2} are of such great magnitude that compartments $\mathbf{M}_2$ and $\mathbf{M}_{3_2}$ maintain an approximately constant ratio (secular equilibrium), equal to a binding potential, p_B. The constant ratio has the effect of reducing the three compartments $\mathbf{M}_2$, $\mathbf{M}_{3_1}$, and $\mathbf{M}_{3_2}$ to two with the relaxation constants k'_2 and k'_{3_1},

$$k'_2 = \frac{k_2}{1 + p_B} \text{ and } k'_{3_1} = \frac{k_{3_1}}{1 + p_B}, \tag{2.219}$$

where p_B is the ratio k_{3_2}/k_{4_2}.

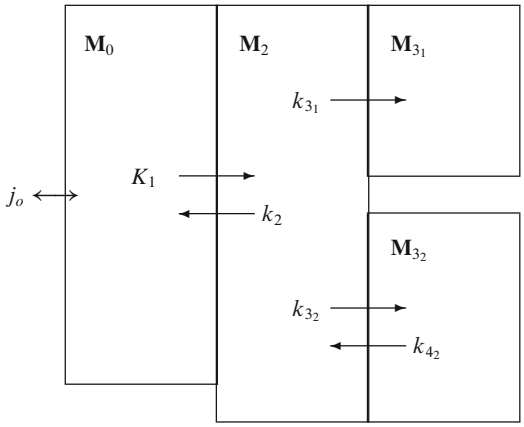

Fig. 2.20 Model of multiple compartments with two parallel compartments and a vascular delivery compartment

In this model, the total uptake of tracer is given by the Blomqvist equation (2.49),

$$m^* = V_o c_a^* + \left[K_1 + V_o(k_2' + k_{3_1}')\right] \int_o^T c_a^* \, dt + K_1 k_{3_1}' \int_o^T \int_o^u c_a^* \, dt \, du - (k_2' + k_{3_1}') \int_o^T m^* \, dt, \tag{2.220}$$

where the symbols have their usual meaning. Equation (2.220) rearranges to the ratio of the areas under the curves as a function of time T,

$$v'^*(T) = \frac{\int_o^T m^* \, dt}{\int_o^T c_a^* \, dt} = \left[\frac{K_1}{k_2' + k_{3_1}'} + V_o\right] + \frac{K_1 k_{3_1}'}{k_2' + k_{3_1}'} \left(\frac{\int_o^T \int_o^u c_a^* \, dt \, du}{\int_o^T c_a^* \, dt}\right) - \left[\frac{m^* - V_o \, c_a^*}{(k_2' + k_{3_1}') \int_o^T c_a^* \, dt}\right], \tag{2.221}$$

where the ratio of the areas under the time-activity curves is v'^*, $K_1 k_{3_1}'/(k_2' + k_{3_1}')$ is K, the net clearance of the ligand, $\int_o^T \int_o^u c_a^* \, dt \, du / \int_o^T c_a \, dt$ is the new time variable Θ'^*, and $(K_1 \int_o^T c_a^* \, dt - m)/[(k_2' + k_{3_1}') \int_o^T c_a^* \, dt]$ represents the monoexponential approach to the time-variable ordinate-intercept $V_g(1 + p_B)$, equal to $K_1 k_2'/(k_2' + k_{3_1}')^2$, where V_g is defined as $K_1 k_2/(k_2 + k_{3_1})^2$,

$$v'^* = K \, \Theta'^* + V_o + V_g \, (1 + p_B) \, (1 - e^{-\alpha \, \Theta'^*}) \tag{2.222}$$

which defines an early phase of slope K/α and ordinate intercept V_o, a late phase of slope K and ordinate intercept $V_o + V_g$, and a monoexponentially changing transition between the two phases. For $k_{3_1} = 0$, (2.220) shrinks to,

$$v'^* = V_o + V_e \, (1 + p_B) \, (1 - e^{-\alpha \, \Theta'^*}), \tag{2.223}$$

where $V_o + V_e(1 + p_B)$ is the steady-state partition volume V, such that $p_B = [(V - V_o)/V_e] - 1$. For $k_{3_1} = 0$ and $p_B = 0$, (2.220) further reduces to,

$$v'^* = V_o + V_e\,(1 - e^{-\alpha\,\Theta'^*}) \tag{2.224}$$

which yields the partition volume $V = V_e + V_o$ at steady-state.

Tissue (Indirect) Forcing Function Although safe, the use of arterial sampling can be an inconvenience to experimental subjects and, in case of patients, can be impossible. Several methods have been proposed for the estimation of binding potentials, using tracer uptake curves in regions of little or no specific binding.

The reference tissue area-under-curves ratio analysis extends the ordinary area-under-curves ratio analysis by integrating the reference region and region of interest tracer uptake curves. The reference region takes the place of the combined delivery and precursor compartments by reversely estimating the tracer concentration in the delivery compartment which yielded the tracer content of the reference region precursor compartment. The new independent variable still has unit of time, and the new dependent variable is the ratio between the integrals of the regions of interest and the integral of the reference region tracer uptake curves (Fig. 2.21).

In the region of reference, the term $m^*_{2_2}$ denotes the tracer content of the precursor compartment of the reference region, $\mathbf{M}_{2_2}$, as function of time. The term $m^*_{[2_1+3_{1_1}+3_{1_2}]}$ denotes the tracer content of the precursor and product compartments

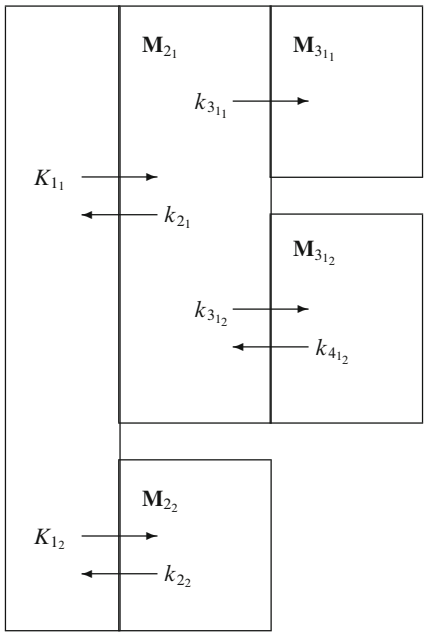

Fig. 2.21 Model of four compartments with two parallel compartments in region of interest, and two compartments in reference region

of the region of interest as a function of time. In the reference region, let the tracer uptake as a function of time be given by (2.18), provided V_o can be claimed to be negligible,

$$m^*_{2_2} = K_{1_2} \int_o^T c^*_{\mathrm{a}}\, \mathrm{d}t - k_{2_2} \int_o^T m^*_{2_2}\, \mathrm{d}t, \tag{2.225}$$

where the symbols have their usual meaning. Note that no initial volume of distribution was assumed in this region. The equation was rearranged to yield an expression of the integral of c_{a},

$$\int_o^T c^*_{\mathrm{a}}\, \mathrm{d}t = \frac{m^*_{2_2}}{K_{1_2}} + \frac{k_{2_2}}{K_{1_2}} \int_o^T m^*_{2_2}\, \mathrm{d}t \tag{2.226}$$

which is integrated once more to yield,

$$\int_o^u \int_o^T c^*_{\mathrm{a}}\, \mathrm{d}t\, \mathrm{d}T = \frac{\int_o^u m^*_{2_2}\, \mathrm{d}T}{K_{1_2}} + \frac{k_{2_2}}{K_{1_2}} \int_o^u \int_o^T m^*_{2_2}\, \mathrm{d}t\, \mathrm{d}T \tag{2.227}$$

for insertion into the equation later.

In the region of interest, a region of specific but reversible accumulation of tracer, the uptake as a function of time is expected to obey the solution to the three-compartment model, (2.49), provided V_o can be claimed to be negligible,

$$\begin{aligned} m_{[2_1+3_{1_1}+3_{1_2}]} = {} & K_{1_1} \int_o^T c^*_{\mathrm{a}}\, \mathrm{d}t + K_{1_1} k'_{3_1} \int_o^T \int_o^u c^*_{\mathrm{a}}\, \mathrm{d}t\, \mathrm{d}u \\ & -(k'_{2_1} + k'_{3_1}) \int_o^T m^*_{[2_1+3_{1_1}+3_{1_2}]}\, \mathrm{d}t, \end{aligned} \tag{2.228}$$

where again the symbols have their usual meaning (for example $k'_{2_1} = k_{2_1}/(1+p_{\mathrm{B}})$ where p_{B} is the binding potential of the tracer for rapidly reversible accumulation in a compartment other than the one responsible for the relaxation constant $k_{3_{1_1}}$). Insertion of (2.226) and (2.227) yields:

$$\begin{aligned} m_{[2_1+3_{1_1}+3_{1_2}]} = {} & R_1 m^*_{2_2} + R_1 (k_{2_2} + k'_{3_{1_1}}) \int_o^T m^*_{2_2}\, \mathrm{d}t + R_1\, k_{2_2}\, k'_{3_{1_1}} \\ & \times \int_o^T \int_o^u m^*_{2_2}\, \mathrm{d}t\, \mathrm{d}u - (k'_{2_1} + k'_{3_{1_1}}) \int_o^T m^*_{[2_1+3_{1_1}+3_{1_2}]}\, \mathrm{d}t, \end{aligned} \tag{2.229}$$

where R_1 symbolizes the K_{1_1}/K_{1_2} ratio. The following derivations assume a short phase in which tracer concentrations, c^*_a, in the vascular bed are significant. During this phase, transfer from the vascular bed to tissue is assumed to dominate, and

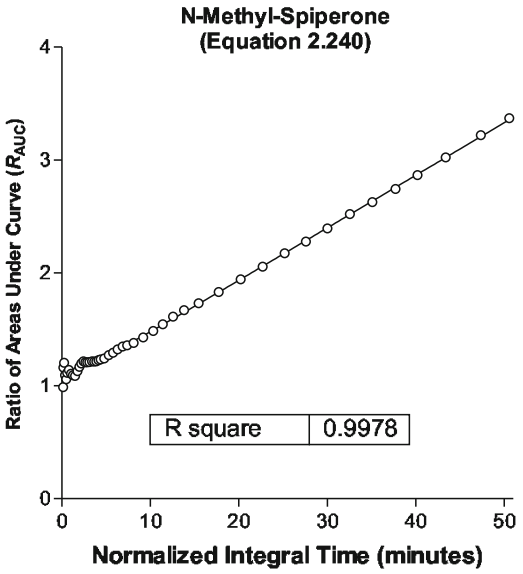

Fig. 2.22 Reference region areas under curves ratio analysis according to (2.240) of tracer *N*-methylspiperone (NMSP) uptake into human striatum in vivo, assumed to be mediated by high-affinity binding to dopamine receptors. Slope is 0.0460 min^{-1} (s.e. ± 0.0005), R_1 is 1.11 ± 0.01, and α is 0.2 ± 0.06

other transfers are assumed negligible. Thus, during this phase, the ratio of tracer mass in the region of interest to that in the reference region is K_{1_1}/K_{1_2}, or R_1. Following this initial phase, is a second in which c_a^* is assumed negligible and the processes ignored in the first phase are assumed to dominate. The second phase, called washout, begins at $t = 0$ with $m^*_{[2_1+3_{1_1}+3_{1_2}]}(0)/m_2^*(0)$ equal to R_1. It is further assumed that $m^*_{3_{1_1}}(0) = 0$ and that $k_{2_1}/k_{2_2} = K_{1_1}/K_{1_2}$ (Fig. 2.22).

To compute the ratio of the contents of tissue of interest relative to the reference tissue as a function of time, transformed time variables are generated from the reference tissue curve in analogy with the definitions of Θ^* and Θ'^* (2.213),

$$\theta^* = \left[\frac{\int_o^T m^*_{2_2}\, \mathrm{d}t}{m^*_{2_2}} \right] \tag{2.230}$$

and

$$\theta'^* = \left[\frac{\int_o^T \int_o^u m^*_{2_2}\, \mathrm{d}t\, \mathrm{d}u}{\int_o^T m^*_{2_2}\, \mathrm{d}t} \right] \tag{2.231}$$

and dividing by the integral of the tracer accumulation in the reference region, the following analog of (2.240) is obtained,

$$\rho^* = \frac{\int_o^T m^*_{[2_1+3_{1_1}+3_{1_2}]}\,\mathrm{d}t}{\int_o^T m^*_{2_2}\,\mathrm{d}t} = \left(\frac{k_{2_1}k_{3_{1_1}}}{k_{2_1}+k_{3_{1_1}}}\right)\theta'^* + R_1\left(\frac{k_{2_2}+k'_{3_{1_1}}}{k'_{2_1}+k'_{3_{1_1}}}\right)\left[1-\frac{\left(\frac{m^*_{[2_1+3_{1_1}+3_{1_2}]}}{R_1\,m^*_{2_2}}-1\right)}{\left(k_{2_2}+k'_{3_{1_1}}\right)\,\theta^*}\right], \tag{2.232}$$

where ρ^* is defined as the ratio between the contents of the region of interest and the reference region as function of the transformed time variable. The following substitutions are based on compartment modeling, which will reduce (2.232) to a more manageable form. For the ratio between the rates of washout from the region of interest and the reference region, the following linked differential equations are solved,

$$\frac{\mathrm{d}m^*_{[2_1+3_{1_2}]}}{\mathrm{d}t} = -(k'_{2_1}+k'_{3_{1_1}})\,m^*_{[2_1+3_{1_2}]},$$

$$\frac{\mathrm{d}m^*_{3_{1_1}}}{\mathrm{d}t} = k'_{3_{1_1}}\,m^*_{2_1}$$

and

$$\frac{\mathrm{d}m^*_{2_2}}{\mathrm{d}t} = -k_{2_2}\,m^*_{2_2} \tag{2.233}$$

from which follows the solution for $m^*_{[2_1+3_{1_1}+3_{1_2}]} = m^*_{[2_1+3_{1_2}]} + m^*_{3_{1_1}}$,

$$\frac{m^*_{[2_1+3_{1_1}+3_{1_2}]}}{m^*_{2_2}} - R_1 = R_1\left[\left(\frac{k'_{3_{1_1}}}{k'_{2_1}+k'_{3_{1_1}}}\right)\mathrm{e}^{k_{2_2}T} + \left(\frac{k'_{2_1}}{k'_{2_1}+k'_{3_{1_1}}}\right)\mathrm{e}^{(k_{2_2}-k'_{2_1}-k'_{3_{1_1}})\,T}-1\right]. \tag{2.234}$$

The second substitution is the result of the wash-out of $m^*_{2_2}$, such that

$$\theta^* \cong \frac{\mathrm{e}^{k_{2_2}T}-1}{k_{2_2}}, \tag{2.235}$$

where k_{2_2} is the wash-out rate or fractional clearance of tracer from the reference region, which is valid when (2.233) hold. With the substitutions, the following intermediate equation arises,

$$\rho^* = \left(\frac{k_{2_1} k_{3_{1_1}}}{k_{2_1} + k_{3_{1_1}}}\right) \theta'^* + R_1 \frac{k_{2_2} + k'_{3_{1_1}}}{k'_{2_1} + k'_{3_{1_1}}} \times \left[1 - \frac{k_{2_2}\, k'_{2_1}}{(k_{2_2} + k'_{3_{1_1}})(k'_{2_1} + k'_{3_{1_1}})}\right.$$
$$\left. \times \left(\frac{1 - \mathrm{e}^{-(k_{2_2} - k'_{2_1} - k'_{3_{1_1}})\, T}}{1 - \mathrm{e}^{-k_{2_2} T)}}\right) \mathrm{e}^{-(k'_{2_1} + k'_{3_{1_1}})\, T} - \frac{k_{2_2}\, k'_{3_{1_1}}}{(k_{2_2} + k'_{3_{1_1}})(k'_{2_1} + k'_{3_{1_1}})}\right]. \tag{2.236}$$

By making the substitution, justified by the empirical observation that, for T between 0 and 100, for the radiotracer raclopride, and for k_{2_2}, k'_{2_1}, and $k'_{3_{1_1}}$ within two standard deviations of the averages shown in Table 2.2, the left hand side is log linear,

$$\left(\frac{k_{2_2} - k'_{2_1} - k'_{3_{1_1}}}{k_{2_2}}\right) \mathrm{e}^{-\alpha\, \theta'^*} \cong \left(\frac{1 - \mathrm{e}^{-(k_{2_2} - k'_{2_1} - k'_{3_{1_1}})\, T}}{1 - \mathrm{e}^{-k_{2_2}\, T)}}\right) \mathrm{e}^{-(k'_{2_1} + k'_{3_{1_1}})\, T} \tag{2.237}$$

the operational equation is derived,

$$\rho^* = \left(\frac{k_{2_1} k_{3_{1_1}}}{k_{2_1} + k_{3_{1_1}}}\right) \theta'^* - \frac{R_1\, k_{2_2}\, k'_{3_{1_1}}}{(k'_{2_1} + k'_{3_{1_1}})^2}$$
$$+ \frac{R_1}{k'_{2_1} + k'_{3_{1_1}}} \left[k_{2_2} + k'_{3_{1_1}} - k'_{2_1} \left(\frac{k_{2_2}}{k'_{2_1} + k'_{3_{1_1}}} - 1\right) \mathrm{e}^{-\alpha\, \theta'^*}\right]. \tag{2.238}$$

Irreversible Accumulation For $p_{\mathrm{B}} = 0$, (2.238) reduces to,

$$\rho^* = \left(\frac{k_{2_1} k_{3_{1_1}}}{k_{2_1} + k_{3_{1_1}}}\right) \theta'^* + R_1 \left[\frac{k_{3_{1_1}}}{k_{2_1} + k_{3_{1_1}}} + \left(\frac{k_{2_1}}{k_{2_1} + k_{3_{1_1}}}\right) \mathrm{e}^{-\alpha\, \theta'^*}\right]$$
$$+ \left(\frac{k_{2_1}}{k_{2_1} + k_{3_{1_1}}}\right)^2 \left[1 - \mathrm{e}^{-\alpha\, \theta'^*}\right] \tag{2.239}$$

which is symmetrical in k_{2_1} and $k_{3_{1_1}}$ when R_1 is close to unity and θ'^* exceeds a certain minimum. Therefore, the relation does not accurately identify the individual estimates of the two rate constants, which must be inferred from other information.

The steady-state ordinate intercept is an indicator of the relative magnitude of the two rate constants, as shown on the left panel of the graph: A lower intercept is indicative of rate constants of similar magnitudes. The closer to unity the steady-state ordinate intercept is, the more dissimilar the magnitudes of the rate constants are. Thus, as shown in Fig. 2.22, for $k_{3_{1_1}} \ll k_{2_1}$,

$$\rho^* \simeq k_{3_{1_1}}\, \theta'^* + 1 - (1 - R_1)\, \mathrm{e}^{-\alpha\, \theta'^*}. \tag{2.240}$$

On the other hand, for $k_{2_1} \ll k_{3_{1_1}}$, as shown for the tracer N-[^{11}C] methylspiperone (NMSP) on the right panel of graph 4.4.4.3., the slope loses its sensitivity to k_3 but the steady-state ordinate intercept remains close to R_1,

$$\rho^* \simeq k_{2_1}\, \theta'^* + R_1 \left(1 + \frac{k_{2_1}}{k_{3_{1_1}}} \left[\frac{k_{2_1}}{k_{3_{1_1}}} + \left(1 - \frac{k_{2_1}}{k_{3_{1_1}}}\right) \mathrm{e}^{-\alpha\, \theta'^*}\right]\right). \tag{2.241}$$

Thus, only for significantly reduced binding of NMSP, e.g., by blockade of the binding by a pharmacologically active dose of an antagonist, is it possible to show any relation of the slope to the receptor density.

Judged from other studies (Gjedde and Wong 2001), (2.22) shows that the slope is not too far from the known value of $k_2 = K_1/V_\mathrm{e} = 0.1/3\ \mathrm{min}^{-1}$ for NMSP and thus has lost its sensitivity to the magnitude of k_3. A partial but inadequate solution to the problem of estimating k_3 under these circumstances is to use the estimate of α, which is close to the value of $k_{2_1} + k_3$, as shown in (2.237). Assuming this to be the case, k_{2_1} is close to $0.051\ \mathrm{min}^{-1}$ and k_3 close to $0.47\ \mathrm{min}^{-1}$, almost an order of magnitude greater. In principle, the ratio could be the inverse, although this would not be consistent with known estimates of K_1 for NMSP. In this case, it appears to be approximately correct to further simplify (2.240) and (2.241),

$$\rho^* \simeq k\, \theta'^* + 1, \tag{2.242}$$

where it is unknown whether k is closest to k_{2_1} or to $k_{3_{1_1}}$ when R_1 is unity and θ'^* exceeds a certain minimum.

Reversible Accumulation When it is known a priori that the tracer is subject to completely reversible accumulation, the relaxation constant $k_{3_{1_1}}$ is zero. As shown in Fig. 2.23, the comprehensive Equation (2.238) then reduces to,

$$\rho^* = 1 + p_\mathrm{B}\left(1 - \mathrm{e}^{-\alpha\, \theta'^*}\right) + (R_1 - 1)\ \mathrm{e}^{-\alpha\, \theta'^*} \tag{2.243}$$

which for $R_1 = 1$ becomes,

$$\rho^* = 1 + p_\mathrm{B}\left(1 - \mathrm{e}^{-\alpha\, \theta'^*}\right) \tag{2.244}$$

which is shown in the graph later (Fig. 2.23 for raclopride. The results of applying this analysis to multiple subjects is listed in Table 2.4. Although the result is visually satisfying, there is reason to be cautious about the many assumptions underlying the analysis and plot, known colloquially as Estimation of Reversible Ligand Binding and Receptor Density (ERLiBiRD).

2.3.5 Deconvolution of Response Function by Linearization

The descriptive graphical analyses reduce the number of apparent variables by lumping the primary variables. They provide precise and often reasonably accurate

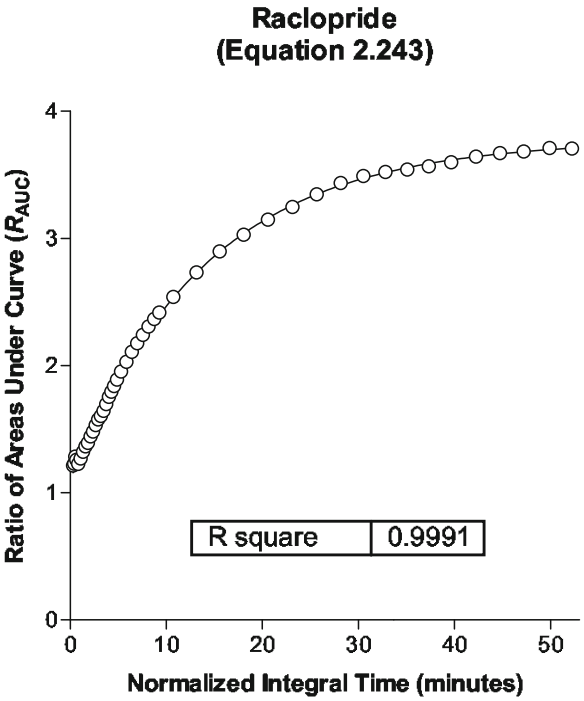

Fig. 2.23 Reference region areas-under-curves ratio analysis of reversible tracer raclopride uptake into human striatum in vivo, assumed to be mediated by medium-affinity binding to dopamine receptors. Binding potential estimate is 2.8 (s.e., $\pm$ 0.01, R_1 is 1.08 $\pm$ 0.01, and α is 0.072 $\pm$ 0.001)

illustrations of transient kinetic processes of brain uptake and metabolism. One great advantage of the methods is the ease with which they reveal key features of kinetic processing, which can be invisible in more conservative presentations of uptake data. A disadvantage is the compounding comminution of dependent and independent variables, which yields a potential bias (Logan et al. 2001).

The apparent clearance as a function of time of circulation is defined as:

$$\kappa_i^* = \frac{m_i^*(T)}{\int_o^T c_a^* \, dt},$$

and the apparent residence time in the precursor or exchange compartment has previously been defined as:

$$\theta_i^* = \frac{\int_o^T m_i^* \, dt}{m_i^*(T)}$$

which are useful when they can be determined directly from the timed measurements of c_a^* and m^* as functions of time, as described earlier.

Vascular Reference

Single-Compartment Linearization For the single-compartment tracer model, the linear plots arising from the application of the lumped variables to (2.17) roughly divide into negative and positive slope plots. In this model, $m^* = m^*_{2_1}$. The *negative-slope* plots include the "clearance" plot (equation 37 in Gjedde 1982; equation 3 in Cumming et al. 1993), Also see footnote 8. which relates the ratio between the product and the substrate integral to the ratio between the product and substrate integrals, as in the equation,

$$\kappa^*_e(T) = K_{1_1} - k_{2_1}\, v'^*_e(T), \tag{2.245}$$

where $v'^*_e(T)$ (2.214) is the apparent partition volume. The reciprocal "ratio" plot (Gjedde et al. 2000),

$$v'^*_e(T) = V_\mathrm{e} - \frac{1}{k_{2_1}}\, \kappa^*_e(T), \tag{2.246}$$

where V_e is the precursor's partition volume. The *positive-slope* plots include the "reciprocal clearance" plot (equation 36 in Gjedde 1982), which relates the ratio between the precursor integral and the product to the ratio between the product integral and the product, the latter equal to the transit time of the product through the product pool, as in the equation,

$$\frac{1}{\kappa^*_e(T)} = \frac{\theta^*_e(T)}{V_\mathrm{e}} + \frac{1}{K_{1_1}}, \tag{2.247}$$

where $1/\kappa^*$ is a reciprocal clearance and k_{2_1}/K_{1_1} is the reciprocal partition volume. The equation was reversed by Logan et al. (1990) as the Logan plot (Logan et al. 1990),

$$\theta^*_e(T) = \frac{V_\mathrm{e}}{\kappa^*_e(T)} - \frac{1}{k_{2_1}}, \tag{2.248}$$

where the positive slope is the partition volume. The third positive-slope equation is the "reciprocal time" plot (equation 2 in Reith et al. 1990), which relates the ratio between the precursor and the product integral to the ratio between the integrals of the precursor and product (Fig. 2.24),

$$\frac{1}{\theta^*_e} = \frac{K_{1_1}}{v'^*_e(T)} - k_{2_1}, \tag{2.249}$$

where the slope is the rate constant of the unidirectional clearance. The most commonly used of these pseudo-linear relations are the Logan plot for the estimation of steady-state volumes of distribution, and the plot of Gjedde (1982) and Cumming et al. (1993) for the estimation of the rates of enzymatic reaction. The plots were originally derived to allow information from multiple experiments to be jointly analyzed, because the ratios eliminate differences of scale among the experiments. The advent of positron emission tomography made the use of the unilinearized plots obsolete, except in the cases in which the number of regressions made the non- or multilinear regressions computationally prohibitive.

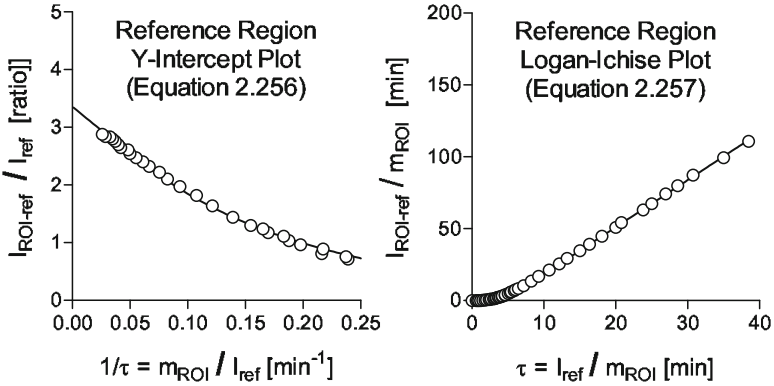

Fig. 2.24 Pseudo-linear reference region plots of binding of tracer raclopride to dopamine receptors in striatum are linear only after steady-state between precursor and delivery compartments, averages of 13 healthy volunteers. In both cases, α is 0.30 min^{-1} and k'_{2_1} is 0.68 min^{-1}, with binding potentials are listed in Table 2.3

Two-Compartment Linearization For the two-compartment models, (2.74) and (2.216) are replaced by (2.18),

$$\frac{\int_o^T m^* \, \mathrm{d}t}{\int_o^T c_\mathrm{a}^* \, \mathrm{d}t} = \left(\frac{K_{1_1}}{k_{2_1}} + V_o\right) - \left(\frac{m^* - V_o \, c_\mathrm{a}^*}{k_{2_1} \int_o^T c_\mathrm{a}^* \, \mathrm{d}t}\right) \tag{2.250}$$

which yields the negative slope "ratio" plot (Gjedde et al. 2000) for times great enough to reduce the term V_o/Θ^* to zero,

$$v^*(T) = (V_\mathrm{e} + V_o) - \left(\frac{1}{k_{2_1}}\right)\kappa^*, \tag{2.251}$$

where the ordinate intercept is $V_\mathrm{e} + V_o$ and the slope is $-1/k_{2_1}$ when the term V_o/v^* approximates zero. The alternative slope or Logan plot follows from the rearrangement of (2.251),

$$\theta^*(T) = (V_\mathrm{e} + V_o)\left(\frac{1}{\kappa^*(T)}\right) - \left(\frac{1}{k_{2_1}}\right) \tag{2.252}$$

which has the slope $V_\mathrm{e} + V_o$ and the ordinate intercept $-1/k_{2_1}$.

Tissue Reference

The reparameterization allows the deconvolution to proceed by linearization. Thus, for $k_{3_{1_1}} = 0$, provided $K_{1_1}/k_{2_1} = K_{1_2}/k_{2_2}$, (2.238) reduces to,

$$\int_o^T m^*_{[2_1+3_{1_1}+3_{1_2}]}\,\mathrm{d}t \;=\; (1+p_\mathrm{B})\int_o^T m^*_{2_2}\,\mathrm{d}t - \left[\frac{m^*_{[2_1+3_{1_1}+3_{1_2}]} - R_1\, m^*_{2_2}}{k'_{2_1}}\right] \tag{2.253}$$

which can be linearized in several ways. For $k_{3_{1_1}} = 0$, it also follows from (2.234) that,

$$1 - R_1\,\frac{m^*_{2_2}}{m^*_{[2_1+3_{1_1}+3_{1_2}]}} = 1 - \mathrm{e}^{-(k_{2_2}-k'_{2_1})\,T}, \tag{2.254}$$

such that,

$$\int_o^T m^*_{[2_1+3_{1_1}+3_{1_2}]}\,\mathrm{d}t = (1+p_\mathrm{B})\int_o^T m^*_{2_2}\,\mathrm{d}t - m^*_{[2_1+3_{1_1}+3_{1_2}]}\left[\frac{1-\mathrm{e}^{-(k_{2_2}-k'_{2_1})\,T}}{k'_{2_1}}\right]. \tag{2.255}$$

With its three parameters ($p_\mathrm{B}, R, k'_{2_1}$), (2.253) can be fitted with nonlinear regression analysis, but (2.254) and (2.255) can be further rearranged to yield approximately linear relationships, as shown in Fig. 2.24.

Ordinate-Intercept Plot The Ordinate Intercept Plot is obtained from (2.255) by subtracting and dividing with $\int_o^T m^*_{2_2}\,\mathrm{d}t$,

$$\frac{\int_o^T (m^*_{[2_1+3_{1_1}+3_{1_2}]} - m^*_{2_2})\,\mathrm{d}t}{\int_o^T m^*_{2_2}\,\mathrm{d}t} \;=\; p_\mathrm{B} - \frac{m^*_{[2_1+3_{1_1}+3_{1_2}]}}{\int_o^T m^*_{2_2}\,\mathrm{d}t}\left[\frac{1-\mathrm{e}^{-\alpha\tau}}{k'_{2_1}}\right], \tag{2.256}$$

where τ is $\int_o^T m^*_{2_2}\,\mathrm{d}t / m^*_{[2_1+3_{1_1}+3_{1_2}]}$, and $\alpha = 1/\tau$ which is linear with an ordinate intercept of p_B and a slope of $-1/k'_{2_1}$ for times great enough to render the exponential term negligible.

Logan-Ichise Plot Alternatively, (2.255) can be rearranged to yield the slope plot (reminiscent of the tissue reference region version of the Logan plot) by subtracting and dividing with $m^*_{[2_1+3_{1_1}+3_{1_2}]}$,

$$\frac{\int_o^T (m^*_{[2_1+3_{1_1}+3_{1_2}]} - m^*_{2_2})\,\mathrm{d}t}{m^*_{[2_1+3_{1_1}+3_{1_2}]}} \;=\; p_\mathrm{B}\left[\frac{\int_o^T m^*_{2_2}\,\mathrm{d}t}{m^*_{[2_1+3_{1_1}+3_{1_2}]}}\right] - \frac{1-\mathrm{e}^{-\alpha\tau}}{k'_{2_1}} \tag{2.257}$$

which is linear with a slope of p_B and an ordinate intercept of $-k'_{2_1}$ for times great enough to render the exponential term negligible.

Table 2.1 Kinetics of enzyme-substrate compound of peroxidase

Symbol	Mean	Unit
k_{on}	0.6	min^{-1} nM^{-1}
k_{off}	12	min^{-1}
k_{in}	252	min^{-1}
K_d	20	nM
K_M	440	nM

2.4 Application of Relaxation Constants

2.4.1 Peroxidation

The original Michaelis–Menten formulation of enzymatic action required approximate steady-state between the ligands in compartments $\mathbf{M_1}$ and $\mathbf{M_2}$. An approximate steady-state exists between these two compartments when $k_{in} \ll k_{off}$. Briggs and Haldane (1925) showed that the formulation is valid also when $k_{in} \gg k_{off}$, which appears to be the case for many enzymes. Estimates of the relaxation constants tend to confirm that magnitudes of K_M greatly exceed the magnitudes of K_d for most enzymes. Chance (1943) studied the enzyme peroxidase and observed that the dissociation constant was only 4.5% of the Michaelis constant, as shown in Table 2.1, indicating that only this small fraction of the molecules do not change into the product. This observation means that the maximum rate is different for the precursor and the product.

2.4.2 Dopaminergic Neurotransmission

Dopamine Receptor Binding Constants

Analysis of tracer [^{11}C]raclopride binding to dopamine receptors in the putamen region of the neostriatum of healthy volunteer subjects by means of standard nonlinear regression of (2.43) (assuming V_1 to have the value zero) to measurements of the time courses of tracer accumulation in arterial blood and a region of interest in the brain ("putamen") yielded the estimates listed in Table 2.2. The estimates of $V_e = K_1/k_2$ (2.51) and $p_B = V_e\,[1 + (k_3/k_4)]$ (2.52) were calculated from the in-

Table 2.2 Tracer raclopride compartmental relaxation constants ($n = 13$) for binding to dopamine $D_{2,3}$ receptors in putamen of human neostriatum (Gjedde and Wong 1990)

Constant	K_1	k_2	k_3	k_4	V_e	p_B
Unit	ml g^{-1} min^{-1}	min^{-1}	min^{-1}	min^{-1}	ml g^{-1}	ratio
Mean estimate	0.16	0.49	0.37	0.100	0.34	3.8
Standard error	0.01	0.03	0.02	0.008	0.02	0.2

Table 2.3 Tracer raclopride binding potential at dopamine $D_{2,3}$ receptors in human striatum, estimated by multiple methods

Analysis	Regression		Differentiation		Temporal transformation		Linearization	
Equation	2.43	2.253	2.208	2.210	2.243	2.243	2.256	2.257
Material	Individual subjects ($n = 13$)					Population average		
Mean estimate	3.8	3.2	3.3	3.5	3.0	2.9	3.3	3.3
Standard error	0.2	0.1	0.1	0.2	0.1	0.01	0.02	0.01

dividual estimates of the clearance and relaxation constants. When calculated from the average estimates, the binding potential (p_B) had the value 3.5, indicating some noise-dependent bias also of the conventional nonlinear regression analysis. It may be appropriate to regard this value as the unbiased "gold" standard.

Dopamine Receptor Binding Potential

Other analyses of tracer [^{11}C]raclopride binding to dopamine receptors in the putamen region of the neostriatum of the healthy volunteer subjects yielded slightly different values of the binding potential at the dopamine D_2 and D_3 receptors, to which raclopride binds. The results of the different approaches are shown in Table 2.3. The table confirms that estimates vary according to the regression method used to obtain the results. Compared to the previously identified "gold" standard of a binding potential of 3.5, the Differentiation and Linearization methods, the latter applied to population averages, yield the closest results.[3]

Comprehensive Model of Dopaminergic Neurotransmission

To examine the ability of compartmental modelling to reveal the role of individual relaxation constants on the regulation of the turn-over of molecules in a specific system of brain biochemistry, we have combined the known elements of dopaminergic neurotransmission in the striatum of the brain. The model consists of the following compartments: The tyrosine compartment being fed from the blood stream by the blood–brain barrier facilitated diffusion transporter, the dopa compartment being fed by tyrosine hydroxylase and decaying both to the blood stream, to 3-*O*-methyldopa, and to the main conduit in the form of dopa decarboxylase to dopamine. The intracellular dopamine department is also fed by the dopamine transporters linking the extracellular and intracellular dopamine compartments. One fraction of the intracellular dopamine is transported into and concentrated in the vesicles and subsequently

[3] "Individual subjects" and "population average" refer to results averaged from regression to 13 individual observations ("individual subjects"), or single result from population averaged observation ("population average"). Averaging removes noise and leads to substantially but unrealistically lowered standard errors.

Table 2.4 Relaxation constants of dopamine turnover

Enzyme or transporter	Relaxation constant	Estimate (min^{-1})
Tyrosine hydroxylase (*secondary flux generator*)	k_{TH}	0.005
DOPA decarboxylase	k_{DDC}	1
Monoamine oxidase	k_{MAO}	20
Dopamine vesicular transporter	k_{VET}	50
Dopamine release (*primary flux generator*)	k_{rel}	0.015
Dopamine diffusion from synapse	k_D	125
Dopamine plasma membrane transporter	k_{DAT}	1,000
LNAA transporter (Tyrosine)	$k_{AT_{TH}}$	0.06
LNAA transporter (DOPA)	$k_{AT_{DOPA}}$	0.05
LNAA transporter (3-*O*-Methyl-DOPA)	$k_{AT_{3OMD}}$	0.2
Catechol-*O*-Methyl-transferase (DOPA)	$k_{COMT_{DOPA}}$	0.03
Catechol-*O*-Methyl-transferase (DOPAC)	$k_{COMT_{DOPAC}}$	0.03
Choriod plexus anion transporter	k_{CSF}	0.04

released to the intrasynaptic cleft, whence the dopamine diffuses to the extrasynaptic space. From the extrasynaptic space it returns to the intracellular space by means of the dopamine transporters' facilitated diffusion. Another fraction of the intracellular dopamine is converted to DOPAC by the monoamine oxidase enzyme. DOPAC in turn is 3-*O*-methylated to homovanillic acid (HVA).

At steady-state, the system is fully described by two out of three variables, e.g., the relaxation constants and the flux through the system, which together define the compartment contents. To calculate the compartment contents, and thus to describe the system in full, tracer measurements of relaxation constants and net flux through the dopamine metabolic pathway were combined to yield the missing compartment contents. The relaxation constants applied to the analysis of dopamine turnover are listed in Table 2.4, and the resulting compartment contents and concentrations are listed in Table 2.5.

The values of the relaxation constants were acquired or calculated on the basis of their definitions. Note that the flux generating steps have relaxation constants of the lowest magnitude of the steps which constitute the pathway. In the definitions later, f_b' symbolizes the bidirectionality of the flux, assuming the value of unity for unidirectional flux and the value of zero for a net flux of zero. The symbol σ refers to the occupancy of the substance, and the symbol ς to the occupancy of a noncompetitive activator in the cases of active transport or an agonist in the cases of receptor binding.

Tyrosine The large neutral amino acid (LNAA) transporter of the blood–brain barrier transports tyrosine by facilitated diffusion from the circulation. The transporter is 95% saturated with the many LNAA in the circulation. However, this competition does not affect the dopamine turnover, as most of tyrosine continues into proteins, and as the entry into the monoamine synthetic pathways is regulated by the activity

Table 2.5 Contents and concentrations of dopaminergic metabolites

Metabolite	Content (nmol g^{-1})	Concentration (μM)	Volume (ml g^{-1})
Tyrosine	56	190	0.300
DOPA	0.3	0.4	0.800
3OMD	0.06	0.075	0.800
Free intracellular DA	0.015	2	0.0075
Vesicular DA	48	60,000	0.0008
Intrasynaptic DA	0.006	7.5	0.0008
Extrasynaptic DA	0.00075	0.005	0.150
Total DA	48		
DA dissociation constant ($K_{d_{DA}}$)		30	
DA maximum binding capacity (B_{max})	0.03		
Bound DA	0.006		
DOPAC	10		
HVA	7.5		

of tyrosine hydroxylase (TH), which is saturated with tyrosine (2.198). The relaxation constant hence is inversely proportional to the content of tyrosine,

$$k_{TH} \cong \frac{V_{max}^{TH}}{M_{Tyr}} \tag{2.258}$$

which in brain tissue is close to 60 nmol g^{-1} in brain tissue. The rate of dopamine turnover has been calculated to be 0.3 nmol g^{-1} min^{-1}, equal to the V_{max} of TH. Thus, the magnitude of k_{TH} is close to 0.005 min^{-1} (Cumming et al. 1998) (Fig. 2.25).

DOPA DOPA (di-hydroxy-phenylalanine) is the product of tyrosine hydroxylation. DOPA is the substrate of aromatic amino acid decarboxylase, also called DOPA decarboxylase (DDC), as well as of the large neutral amino acid transporter of the blood–brain barrier and the enzyme catechol-*O*-methyltransferase (COMT). DDC is unsaturated and the DDC reaction is irreversible, with the relaxation constant,

$$k_{DDC} \cong \frac{V_{max}^{DDC}}{V_{DOPA} K_M^{DDC}}. \tag{2.259}$$

As the enzyme is unsaturated, it is difficult to determine its true activity in vivo. Instead, the relaxation constant of DDC in mammalian brain has been measured directly with labeled substrates of the enzyme in vivo and its magnitude varies from region to region, but the results are suspected of being low because of loss of tracer. In striatum, the measured value ranges from 0.05 to 0.1 min^{-1} but the true value may be as high as 1 min^{-1} (Cumming et al. 1995). In addition to the decarboxylation, DOPA is also subject to transport by the LNAA transporter. The relaxation constant of this process, k_{AT}, averaged 0.05 min^{-1} in vivo (Cumming et al. 1993),

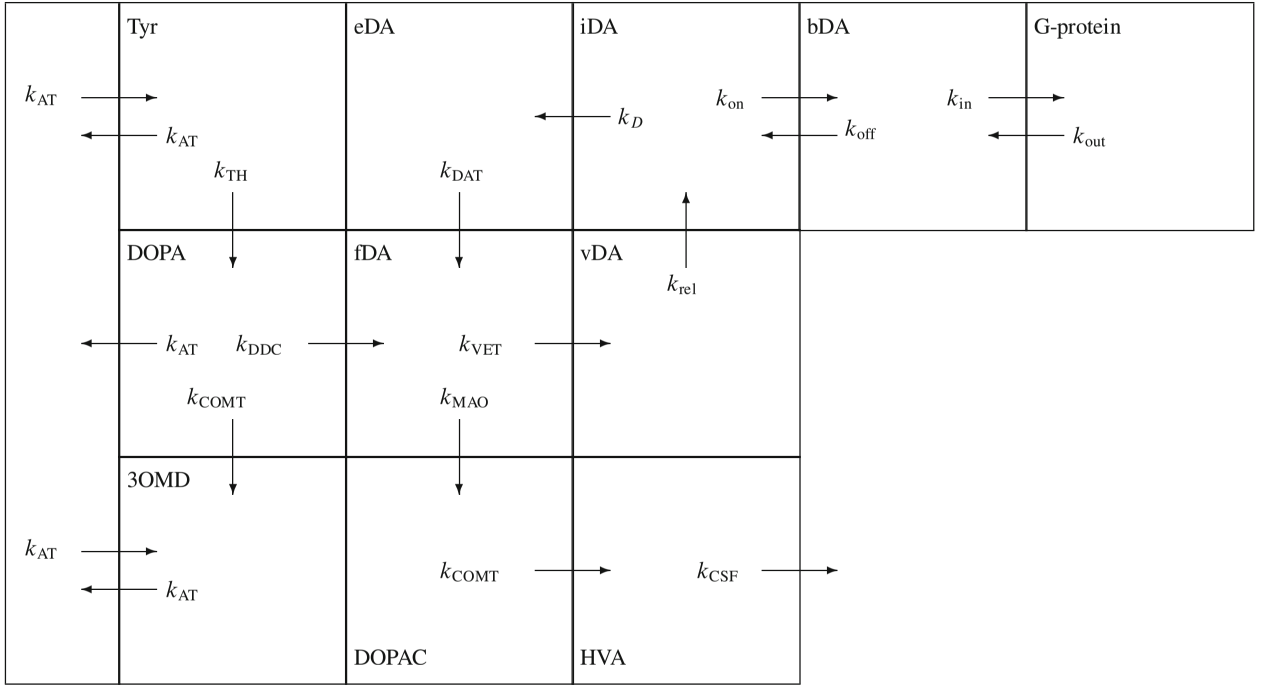

Fig. 2.25 Model of neurotransmitter compartments separated by enzymes (TH, COMT, DDC, and MAO), transporters (AT, VET, and DAT), vesicular release (REL), and intra- to extrasynaptic permeability by passive diffusion (D)

$$k_{\mathrm{AT(DOPA)}} = \frac{f_b{}'\,\sigma_{\mathrm{DOPA}}^{\mathrm{LNAA}}\,T_{\mathrm{max}}^{\mathrm{LNAA}}}{M_{\mathrm{DOPA}}}, \tag{2.260}$$

where $f_b{}'$ is close to unity because of the unidirectional efflux of DOPA from brain tissue. Finally, DOPA is subject to 3-*O*-methylation in the liver and other tissues including brain. The relaxation constant of this process averages about 0.03 min^{-1} in vivo (Cumming et al. 1993),

$$k_{\mathrm{COMT(DOPA)}} = \frac{\sigma_{\mathrm{DOPA}}^{\mathrm{COMT}}\,V_{\mathrm{max}}^{\mathrm{COMT}}}{M_{\mathrm{DOPA}}}. \tag{2.261}$$

3-*O*-methyl-DOPA The 3-*O*-methyl-DOPA (3OMD) generated by COMT in tissues is exchanged with 3OMD in the circulation by means of the neutral amino acid transporter of the blood–brain-barrier. The concentrations of 3OMD in plasma and tissues are likely to be similar because of the comparatively high relaxation constant of the transporter, $k_{\mathrm{AT(3OMD)}}$, which has been measured to average about 0.2 min^{-1} (2.194),

$$k_{\mathrm{AT(3OMD)}} = \frac{f_b{}'\,\sigma_{\mathrm{3OMD}}\,T_{\mathrm{max}}^{\mathrm{LNAA}}}{M_{\mathrm{3OMD}}}. \tag{2.262}$$

Intracellular Dopamine As the product of DDC and dopamine transporter action, intracellular dopamine (f DA) is the junction of two metabolic paths, one involving the vesicular transporter (VET) in the membranes of vesicles, driven by proton antiport, the other involving monoamine oxidase (MAO),

$$k_{\mathrm{MAO}} = \frac{\sigma_{\mathrm{fDA}}^{\mathrm{MAO}}\,V_{\mathrm{max}}^{\mathrm{MAO}}}{M_{\mathrm{fDA}}}, \tag{2.263}$$

where the unidirectionality of the reaction renders $f_b{}'$ equal to unity. The relaxation constant of MAO has been estimated as the ratio between the V_{max} and the K_{M} in tissue homogenates and was found to be approximately 20 min^{-1} (Azzaro et al. 1985). To match the known dopamine turnover rate of 0.3 nmol g^{-1} min^{-1}, the intracellular dopamine content (outside vesicles) must be equal to 0.015 nmol g^{-1}, corresponding to an intracellular dopamine concentration of 2 μM. This concentration is consistent with the free intracellular dopamine concentration in giant squid neurons of the order of 1 μM (Chien et al. 1990). Also acting on the intracellular dopamine, the vesicular dopamine transporter actively trasfers dopamine to the vesicles in symport with hydrogen ions, which act as noncompetitive activators (Johnson and Scarpa 1979),

$$k_{\mathrm{VET}} = \frac{f_b{}'\,\sigma_{\mathrm{fDA}}^{\mathrm{VET}}\,\varsigma_{\mathrm{H+}}^{\mathrm{VET}}\,T_{\mathrm{max}}^{\mathrm{VET}}}{M_{\mathrm{fDA}}}. \tag{2.264}$$

The relaxation constant of the vesicular transporter (VET) was calculated from the rate of release of dopamine from the vesicles. To be consistent with a lower limit of dopamine release from vesicles (see later), k_{VET} must average at least 50 min^{-1},

acting on the intracellular content of 0.015 nmol g^{-1} for a flux of 0.75 nmol g^{-1} min^{-1}. Then, the total influx of dopamine into the free intracellular compartment must be at least 1.05 nmol g^{-1} min^{-1}, of which an amount of 0.75 nmol g^{-1} min^{-1} reenters the vesicles and an amount of 0.3 nmol g^{-1} min^{-1} undergoes monoamine oxidation.

Vesicular Dopamine Most of the tissue dopamine, 48 nmol g^{-1}, is believed to reside in vesicles in the dopaminergic terminals. Quanta of the vesicular dopamine are released to the intrasynaptic space in response to action potential arrival. The relaxation constant of the release of dopamine from vesicles in the baseline state is the ratio between the dopamine release rate of 0.75 nmol g^{-1} min^{-1} and the vesicular dopamine (vDA) content of 48 nmol g^{-1} (see (2.111)),

$$k_{\text{rel}} = \frac{J_{\text{vDA}}^{\text{rel}}}{M_{\text{vDA}}}, \tag{2.265}$$

where the baseline state is considered the lower limit of the half-life of total dopamine in the tissues with active dopaminergic neurotransmission. This halflife is close to 45 min, (Cumming et al. 1999), corresponding to a rate constant of 0.015 min^{-1}.

Intrasynaptic Dopamine Intrasynaptic dopamine (iDA) is balanced among the processes of vesicular release, receptor binding, and passive diffusion to the extrasynaptic space. The passive diffusion is driven by the concentration gradient established by the dopamine transporters. The compartment decays by diffusion to the extrasynaptic space, with the relaxation constant,

$$k_D = \frac{A\sqrt{kD}}{V_{\text{iDA}}}, \tag{2.266}$$

where k is the rate constant of the concentration dependent removal of the dopamine, catalyzed by the dopamine transporter facing the extrasynaptic space (see later), D the dopamine diffusion coefficient, A the area of the interface between the intra- and extrasynaptic compartments, and V_{iDA} is the volume of the intrasynaptic compartment. The dopamine content of the compartment was assumed to be 6 pmol g^{-1} in agreement with the binding potential of unity derived from one study of dopamine binding (see later), corresponding to a relaxation constant of 125 min^{-1} for a baseline dopamine flux of 0.75 nmol g^{-1} min^{-1}.

Extrasynaptic Dopamine Extrasynaptic dopamine (eDA) is a weighted average of diffusion profiles established by the clearance of dopamine from the intrasynaptic space and facilitated diffusion mediated by the dopamine transporters surrounding the extrasynaptic space. The dopamine transport actively transports dopamine in proportion to the sodium ion gradient. The sodium ion concentration provides the noncompetitive activation which raises the maximum transport capacity in proportion to the sodium ion concentration, as expressed operationally by the difference

between the magnitudes of the sodium ion occupancy (ς_{Na+}) on the two sides of the membrane. The relaxation constant of this compartment is (2.138) and 2.194),

$$k_{DAT} = f_b{}' \frac{A\sqrt{kD}}{V_{eDA}} \left[\frac{1 - e^{-V_{eDA}\sqrt{k/D}/A}}{1 - f_b{}' \left(1 - \frac{1 - e^{-[V_{eDA}\sqrt{k/D}/A]}}{V_{eDA}\sqrt{k/D}/A} \right)} \right], \tag{2.267}$$

where $1 - f_b{}'$ is the ratio between the occupancies of the transporter ligand on the two sides of the transporting membrane at the onset of diffusion, i.e., at the interface between the intra- and extrasynaptic spaces (see (2.138)), A is the area of the interface between the intra- and extrasynaptic compartments, V_{eDA} the volume of the extrasynaptoc space, D the dopamine diffusion coefficient in the extrasynaptic space, and k is the relaxation constant of the facilitated transport, defined as (2.128),

$$k = \frac{\overline{P}'_{DAT} S}{V_{eDA}} \tag{2.268}$$

and equal to (2.183),

$$k = \frac{\overline{f_b}' \, \overline{\sigma}_{eDA} \, \overline{\varsigma}_{Na+} \, T_{max}}{M_{eDA}} = \frac{J_{DAT}}{M_{eDA}}, \tag{2.269}$$

where $\overline{f_b}'$ is the weighted average magnitude of $f_b{}'$, $\overline{\sigma}_{eDA}$ the weighted average extracellular dopamine occupancy of the transporter, $\overline{\varsigma}_{Na+}$ the weighted average occupancy of the noncompetitive activator (Na^+), and M_{eDA} is the weighted average extrasynaptic dopamine content. The magnitude was calculated to be 1,000 min^{-1} from the relationships derived later. Because $1 - f_b{}'$ refers to the ratio between the concentrations of free dopamine in the dopaminergic neurons and dopamine in the intrasynaptic space, $f_b{}'$ must be close to unity. When $f_b{}' = 1$, and the steady-state volume ratio $V_{eDA}\sqrt{k/D}/A = V_{eDA}/(A\, l_D$ is represented by the symbol λ, (2.267) reduces to,

$$k_{DAT} = \lambda \left(\frac{A\sqrt{kD}}{V_{eDA}} \right) = \frac{\lambda \, K_o}{V_{eDA}}, \tag{2.270}$$

where λ is a measure of how much larger the extracellular space is than the extrasynaptic volume reached by dopamine diffusion and hence an index of the degree to which the dopamine transport raises the gradient of the diffusion of dopamine in the extracellular space by a factor, which is also the reciprocal of the fraction of the extracellular space reached by dopamine diffusing from the sites of release.

Receptor-Bound Dopamine (bDA) The dopamine occupancy of dopamine's receptors is a function of the intrasynaptic concentration and the receptor dissociation

constants, and the amount of bound dopamine is the product of the maximum binding capacity and the occupancy (2.165),

$$\rho_{B_{\mathrm{iDA}}} = \frac{\sigma'_{\mathrm{iDA}}\, B_{\max}^{\mathrm{DAR}}}{M_{\mathrm{iDA}}}, \tag{2.271}$$

where σ'_{iDA} symbolizes the increased binding due to the higher affinity caused by the binding of GTP-free G-protein. The binding of dopamine to G-protein linked receptors acts as a competitive activation of the G-protein binding, which in turn activates second-messenger systems in the cells (2.177) as in Gjedde and Wong (2001) and Cumming et al. (2002). The average normal dopamine occupancy was assumed to be 20%. With equal amounts of bound and free dopamine, 6 pmol g^{-1} (Borbely et al. 1999), the binding potential is unity.

Dihydroxy-phenyl-acetic acid Dihydroxy-phenyl-acetic acid (DOPAC) is the product of the reaction of dopamine with monoamine oxidase. In turn, DOPAC is the substrate of an irreversible reaction catalyzed by COMT. The relaxation constant of the COMT reaction was argued earlier to be close to 0.03 min^{-1} in vivo (Cumming et al. 1993).

$$k_{\mathrm{COMT(DOPAC)}} = \frac{\sigma_{\mathrm{DOPAC}} V_{\max}^{\mathrm{COMT}}}{M_{\mathrm{DOPA}}}. \tag{2.272}$$

Homovanillic Acid Homovanillic acid (HVA) is the product of the reaction between DOPAC and COMT. HVA is cleared from brain tissue by anionic transport across the choroid epithelium, at a rate estimated to be 0.04 min^{-1} (Cumming et al. 1992),

$$k_{\mathrm{CSF}} = \frac{f_b{}'\, \sigma_{\mathrm{HVA}}^{\mathrm{CSF}}\, \varsigma_{\mathrm{OH}-}^{\mathrm{CSF}}\, T_{\max}^{\mathrm{CSF}}}{M_{\mathrm{HVA}}}. \tag{2.273}$$

Dopamine Turnover

Normal Dopamine Turnover To determine the magnitudes of the relaxation constants and compartments participating in the dopamine turnover, it is necessary to measure the relaxation constants or contents, or both, in vivo. However, not all constants or contents are known yet, in humans or other mammals. The relationships can be used to infer values, which subsequently undergo experimental verification. The values listed in Tables 2.4 and 2.5 are presented as internally consistent examples, to be adjusted in the future, with the aid of the following ratios. The steady-state sum of unbound dopamine in dopaminergec neurons, relative to tyrosine, is,

$$\frac{M_{\mathrm{DA}}}{M_{\mathrm{Tyr}}} = \left(\frac{k_{\mathrm{DDC}}}{k_{\mathrm{MAO}}}\right)\left[\frac{k_{\mathrm{TH}}}{k_{\mathrm{DDC}} + k_{\mathrm{AT}} + k_{\mathrm{COMT}}}\right]\left(1 + \frac{k_{\mathrm{VET}}}{k_{\mathrm{rel}}} + \frac{k_{\mathrm{VET}}}{k_D} + \frac{k_{\mathrm{VET}}}{k_{\mathrm{DAT}}}\right), \tag{2.274}$$

where the free intracellular dopamine is given by:

$$M_{\mathrm{fDA}} = \left(\frac{k_{\mathrm{DDC}}}{k_{\mathrm{MAO}}}\right)\left[\frac{k_{\mathrm{TH}}}{k_{\mathrm{DDC}} + k_{\mathrm{AT}} + k_{\mathrm{COMT}}}\right] M_{\mathrm{Tyr}} = f_{\mathrm{f}}\, M_{\mathrm{Tyr}}, \tag{2.275}$$

the vesicular dopamine by,

$$M_{\mathrm{vDA}} = \left(\frac{k_{\mathrm{DDC}}}{k_{\mathrm{MAO}}}\right)\left[\frac{k_{\mathrm{TH}}}{k_{\mathrm{DDC}} + k_{\mathrm{AT}} + k_{\mathrm{COMT}}}\right]\left(\frac{k_{\mathrm{VET}}}{k_{\mathrm{rel}}}\right) M_{\mathrm{Tyr}} = f_{\mathrm{v}}\, M_{\mathrm{Tyr}}, \tag{2.276}$$

and the intrasynaptic dopamine is given by:

$$M_{\mathrm{iDA}} = \left(\frac{k_{\mathrm{DDC}}}{k_{\mathrm{MAO}}}\right)\left[\frac{k_{\mathrm{TH}}}{k_{\mathrm{DDC}} + k_{\mathrm{AT}} + k_{\mathrm{COMT}}}\right]\left(\frac{k_{\mathrm{VET}}}{k_{D}}\right) M_{\mathrm{Tyr}} = f_{\mathrm{i}}\, M_{\mathrm{Tyr}} \tag{2.277}$$

such that the bound dopamine is,

$$M_{\mathrm{bDA}} = \frac{B_{\max}\, M_{\mathrm{Tyr}}}{M_{\mathrm{Tyr}} + \left(\frac{k_{\mathrm{MAO}}}{k_{\mathrm{DDC}}}\right)\left[\frac{k_{\mathrm{TH}} + k_{\mathrm{AT}} + k_{\mathrm{COMT}}}{k_{\mathrm{TH}}}\right]\left(\frac{k_{D}}{k_{\mathrm{VET}}}\right) K_{\mathrm{d_{DA}}}} = \frac{B_{\max}\, M_{\mathrm{Tyr}}}{M_{\mathrm{Tyr}} + (K_{\mathrm{d_{DA}}}/f_{\mathrm{i}})} \tag{2.278}$$

and the extrasynaptic dopamine is,

$$M_{\mathrm{eDA}} = \left(\frac{k_{\mathrm{DDC}}}{k_{\mathrm{MAO}}}\right)\left[\frac{k_{\mathrm{TH}}}{k_{\mathrm{DDC}} + k_{\mathrm{AT}} + k_{\mathrm{COMT}}}\right]\left(\frac{k_{\mathrm{VET}}}{k_{\mathrm{DAT}}}\right) M_{\mathrm{Tyr}} = f_{\mathrm{e}}\, M_{\mathrm{Tyr}} \tag{2.279}$$

which, as confirmation, yields the correct ratio between intra- and extrasynaptic dopamine,

$$\frac{M_{\mathrm{iDA}}}{M_{\mathrm{eDA}}} = \frac{k_{\mathrm{DAT}}}{k_{D}} = \lambda\, \frac{V_{\mathrm{iDA}}}{V_{\mathrm{eDA}}} \tag{2.280}$$

and hence the ratio between the average bconcentrations of intra- and extrasynaptic dopamine,

$$\frac{C_{\mathrm{iDA}}}{\overline{C}_{\mathrm{eDA}}} = \lambda = 1,500, \tag{2.281}$$

where λ is,

$$\lambda = \frac{L}{l_{\mathrm{D}}} = \sqrt{\frac{\overline{\sigma}_{\mathrm{eDA}}\, \varsigma_{\mathrm{Na+}}\, T_{\max}}{\overline{C}_{\mathrm{eDA}}\, DA/L}} = \sqrt{\frac{J_{\mathrm{DAT}}}{\overline{C}_{\mathrm{eDA}}\, DA/L}} = \sqrt{\frac{D_{\mathrm{app}}}{D}} \tag{2.282}$$

according to which the ratio rises and falls with the occupancy of the dopamine transporter and the length of the diffusion path. The value of lambda suggests that the dopamine transporter accelerates the rate of dopamine removal from the extrasynaptic space by a factor of 2.25×10^6.

Inhibition of Dopamine Transporter Inhibition of dopamine transport will raise both intra- and extrasynaptic dopamine. The change depends on the degree of inhibition of the transporter and hence on the lowering of the apparent dopamine diffusion from the intrasynaptic pool, according to (2.282). A lowering of the effective transport rate to 1% of the normal average will raise intrasynaptic dopamine by a factor of 10 and extrasynaptic dopamine by a factor of 100, as well as extending the extracellular space reached by dopamine by a factor of 10 as well.

http://www.springer.com/978-1-4419-7408-2

Neurokinetics
The Dynamics of Neurobiology in Vivo
Gjedde, A.; Bauer, W.R.; Wong, D.
2011, XVI, 343 p., Hardcover
ISBN: 978-1-4419-7408-2